



AIAA 2000-0295
Fabrication and Testing of the Purdue
Mach-6 Quiet-Flow Ludwieg Tube

Steven P. Schneider
Purdue University
West Lafayette, IN

38th Aerospace Sciences Meeting & Exhibit
10–13 January 2000
Reno, Nevada

Fabrication and Testing of the Purdue Mach-6 Quiet-Flow Ludwig Tube

Steven P. Schneider*
School of Aeronautics and Astronautics
Purdue University
West Lafayette, IN 47907-1282

ABSTRACT

Purdue University is developing a Mach-6 Ludwig tube for quiet-flow operation to high Reynolds number. The aerodynamic and mechanical design were reported on earlier. The design predicts laminar flow to the exit of the 9.5-inch nozzle, at a unit Reynolds number of 3 million per foot. The detailed mechanical design, fabrication, and testing are challenging, since maintenance of a laminar boundary layer on the nozzle wall requires very tight tolerances and uniform mirror finishes. Critical issues in mechanical design and fabrication are discussed, along with results of tests carried out during fabrication. The measurements include contour accuracy, waviness, and roughness. The design and testing of other facility systems are also described: these include the driver-tube heating, and the air filtering and heating equipment.

INTRODUCTION

Hypersonic Laminar-Turbulent Transition

Laminar-turbulent transition in hypersonic boundary layers is important for prediction and control of heat transfer, skin friction, and other boundary layer properties. However, the mechanisms leading to transition are still poorly understood, even in low-noise environments. Applications hindered by this lack of understanding include reusable launch vehicles such as the X-33, high-speed interceptor missiles ([20], [21]), and hypersonic cruise vehicles [1].

Many transition experiments have been carried out in conventional ground-testing facilities over the

past 50 years. However, these experiments are contaminated by the high levels of noise that radiate from the turbulent boundary layers normally present on the wind tunnel walls [8, 33, 32]. These noise levels, typically 0.5-1% of the mean, are an order of magnitude larger than those observed in flight [36, 49]. These high noise levels can cause transition to occur an order of magnitude earlier than in flight [8, 49]. In addition, the mechanisms of transition operational in small-disturbance environments can be changed or bypassed altogether in high-noise environments; these changes in the mechanisms change the parametric trends in transition [36]. For example, linear instability theory suggests that the transition Reynolds number on a 5 degree half-angle cone should be 0.7 of that on a flat plate, but noisy tunnel data showed that the cone transition Reynolds number was about twice the flat plate result. Only when quiet tunnel results were obtained was the theory verified [15]. This is critical, since design usually involves consideration of the trend in transition when a parameter is varied. Clearly, transition measurements in conventional ground-test facilities are generally not reliable predictors of flight performance. *Only the study of controlled disturbances in a controlled quiet environment can produce unambiguous data suitable for development of reliable theory.* Reliable predictive methods will have to be based on estimates of the flight disturbance environment.

Development of Quiet-Flow Wind Tunnels

Only in the last two decades have low-noise supersonic wind tunnels been developed [8, 62]. This development has been difficult, since the test-section wall boundary-layers must be kept laminar in order to avoid high levels of eddy-Mach-wave acoustic radiation from the normally-present turbulent boundary layers. A Mach 3.5 tunnel was the first to be successfully developed at NASA Langley [4]. Langley then developed a Mach 6 quiet nozzle, which

*Associate Professor. Senior Member, AIAA.

¹Copyright ©2000 by Steven P. Schneider. Published by the American Institute of Aeronautics and Astronautics, Inc., with permission.

was used as a starting point for the new Purdue nozzle [11]. Unfortunately, this nozzle was decommissioned due to a space conflict. Langley is also attempting to develop a Mach 8 quiet tunnel [62]; however, the high temperatures required to reach Mach 8 have made this a very difficult and expensive effort. Shakedown of this tunnel continues, several years after first installation; successful operation remains to be achieved (Steve Wilkinson, private communication, Dec. 1999). The new Purdue Mach-6 quiet flow Ludwig tube may be the only operational hypersonic quiet tunnel in the world.

Background of the Purdue Mach-6 Quiet-Flow Ludwig Tube

A Mach-4 Ludwig tube was constructed at Purdue in 1992, using a 4-inch nozzle of conventional design that was obtained surplus from NASA Langley. By early 1994, quiet-flow operation was demonstrated at the low Reynolds number of about 400,000 [45]. Since then, this facility has been used for development of instrumentation and for measurements of instability waves under quiet-flow conditions [58, 57, 40, 44, 43, 42, 22, 23]. However, the low quiet Reynolds number imposes severe limitations; for example, the growth of instability waves under controlled conditions on a cone at angle of attack was only about a factor of 2 [22]. This is far smaller than the factor of $e^9 - e^{11}$ typically observed prior to transition, and small enough to make quantitative comparisons to computations very difficult.

A facility that remains quiet to higher Reynolds numbers was therefore needed. The low operating costs of the Mach-4 tunnel had to be maintained. However, hypersonic operation was needed in order to provide experiments relevant to the hypersonic transition problems described above. Operation at Mach 6 was selected, since this is high enough for the hypersonic 2nd-mode instability to be dominant under cold-wall conditions, and high enough to observe hypersonic roughness-insensitivity effects, yet low enough that the required stagnation temperatures do not add dramatically to cost and difficulty of operation. Reference [47] describes the overall design of the facility, and the detailed aerodynamic design of the quiet-flow nozzle, carried out using the e^N method.

Attached flow should be maintained in the contraction of the nozzle, since the separation bubbles sometimes observed in wind tunnel contractions are generally unsteady, and would transmit noise downstream into the Mach-6 nozzle. Preliminary analyses have suggested that the low-frequency fluctua-

tions present in the Langley Mach-6 quiet nozzle [11] may be caused by such a separation. Therefore, a detailed aerodynamic design of the contraction was also carried out [46]. Reference [46] also supplies a preliminary report on the detailed mechanical design of the nozzle and contraction, which was carried out during 1997-98. This mechanical design is not trivial. The nozzle is 9.5 inches in diameter at the exit, and 8-1/2 feet long, yet the inside surface must be fabricated very accurately, with very tight specifications on contour accuracy, steps and gaps, waviness, and roughness. Any of these flaws can trip the laminar boundary layer on the wall, causing early transition and loss of quiet flow, or generate Mach waves that focus on the centerline and cause marked variations in centerline Mach number. Since there are many possible causes for early transition, careful testing of each possible disturbance source during fabrication will be an essential element in successful development.

The detailed mechanical design of the contraction and nozzle was completed by Dynamic Engineering Inc. (DEI) in late 1998, in cooperation with the author. After some initial tests of fabrication procedures, a purchase order for fabrication of these parts was awarded to DEI in January 1999. Delivery has been delayed by almost one year due to problems fabricating the mandrel for the high-tolerance throat section. Delivery is now scheduled for Fall 2000. This paper will report on many of the critical design details not described in Reference [46].

The Purdue Mach-6 Quiet-Flow Ludwig Tube

Quiet facilities require low levels of noise in the inviscid flow entering the nozzle through the throat, and laminar boundary layers on the nozzle walls. These features make the noise level in quiet facilities an order of magnitude lower than the 0.5 to 3 percent pressure fluctuations typical of conventional facilities. In order to reach these low noise levels, conventional blow-down facilities must be extensively modified. Requirements include a 1 micron particle filter, a highly polished nozzle with bleed slots for the contraction-wall boundary layer, and a large settling chamber with screens and sintered-mesh plates for noise-reduction [8]. To reach these low noise levels in an affordable way, the Purdue facility has been designed as a Ludwig tube [45]. A Ludwig tube is a long pipe with a converging-diverging nozzle on the end, from which flow exits into the nozzle, test section, and second throat (Figure 1).

A diaphragm is placed downstream of the test section. When the diaphragm bursts, a shock wave

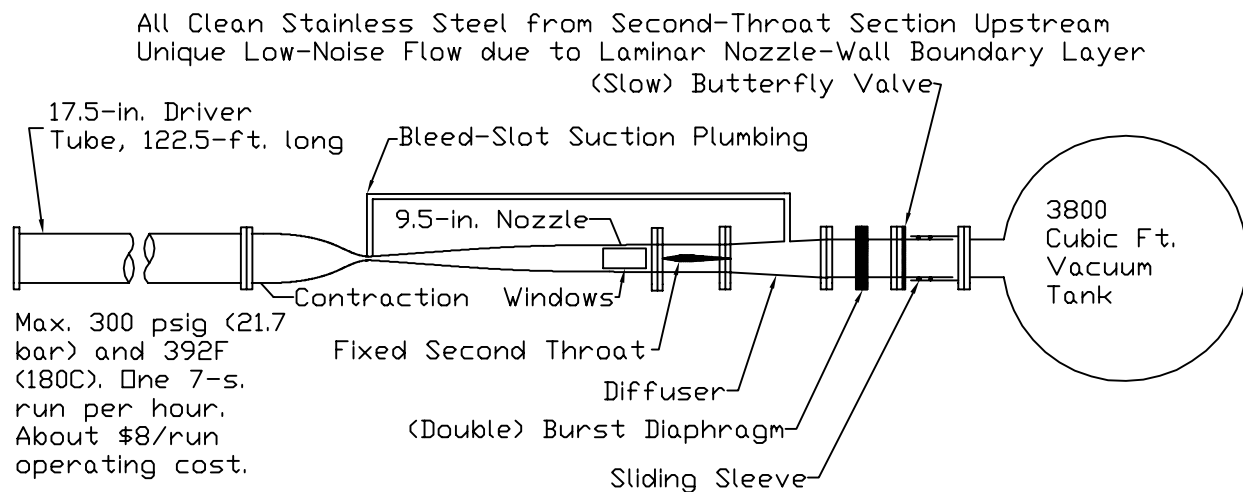


Figure 1: Schematic of Purdue Mach-6 Quiet-Flow Ludwieg Tube

passes downstream, and an expansion wave travels upstream through the test section into the driver tube. The nominal end of the run occurs when the expansion wave has returned to the test section after reflecting from the upstream end of the driver tube. Since the flow remains quiet after the wave reflects, sufficient vacuum can extend the useful run-time to many cycles of expansion-wave reflection, during which the pressure drops quasi-statically [59].

Figure 2 shows the nozzle of the existing facility.

The region of useful quiet flow lies between the characteristics marking the onset of uniform flow, and the characteristics marking the upstream boundary of acoustic radiation from the onset of turbulence in the nozzle-wall boundary layer. A 7.5-deg. sharp cone is also drawn on the figure. The cone is drawn at the largest size for which it is likely to start, according to Schueler [60]. A blunt model of about 3/5 of this size is predicted to start, according to Pope and Goin [35]. Bountin et al. have started a 7-deg. small-bluntness cone with a base diameter of 123 mm (4.83 in.) in a Mach-6 tunnel with a 200-mm diameter (7.87 in.) [13]. Thus, the Schueler-based estimate seems to be reasonable.

The usual quiet-flow length Reynolds number is based on the unit Reynolds number and the length on the centerline between the onset of uniform flow and the first arrival of noise radiated from the nozzle walls. For an axisymmetric nozzle with a nominally uniform transition location, the full quiet uniform-flow region will consist of back-to-back cones, each with a half-angle equal to the Mach angle. Unfortunately, only flat plates and very slender models can make use of the portion downstream of the nozzle

exit. Since neither of these flows is of particular interest, this portion was not thought to be very useful. The present facility therefore places the nozzle sting support immediately downstream of the nozzle exit, to shorten the model sting and reduce the cost of the tunnel.

ROUGHNESS AND WAVINESS IN THE QUIET NOZZLE

The baseline for the Purdue nozzle is the NASA Langley Mach-6 quiet nozzle [10]. The only other hypersonic quiet-flow nozzle is the Langley Mach-8 nozzle which is undergoing shakedown and characterization [62, 63, 3]. Considerable experience has been developed at NASA Langley, using various prototype nozzles primarily at Mach 3.5 and Mach 5. This section describes design issues and test results.

Quiet-flow Reynolds number performance seems to be limited by roughness in the nozzle throat, above throat unit Reynolds numbers of about 1×10^8 , or Mach-6 stagnation pressures of about 100-150 psia, unless extraordinary polishes are achieved (and these are difficult to maintain) [47, p. 7]. With present technology, it seems that useful throat unit Reynolds numbers will be limited to about $1 \times 10^8/m$, or that useful Mach-6 stagnation pressures will be limited to 150 to 200 psia. However, achieving this level of performance will still require very careful attention to detail.

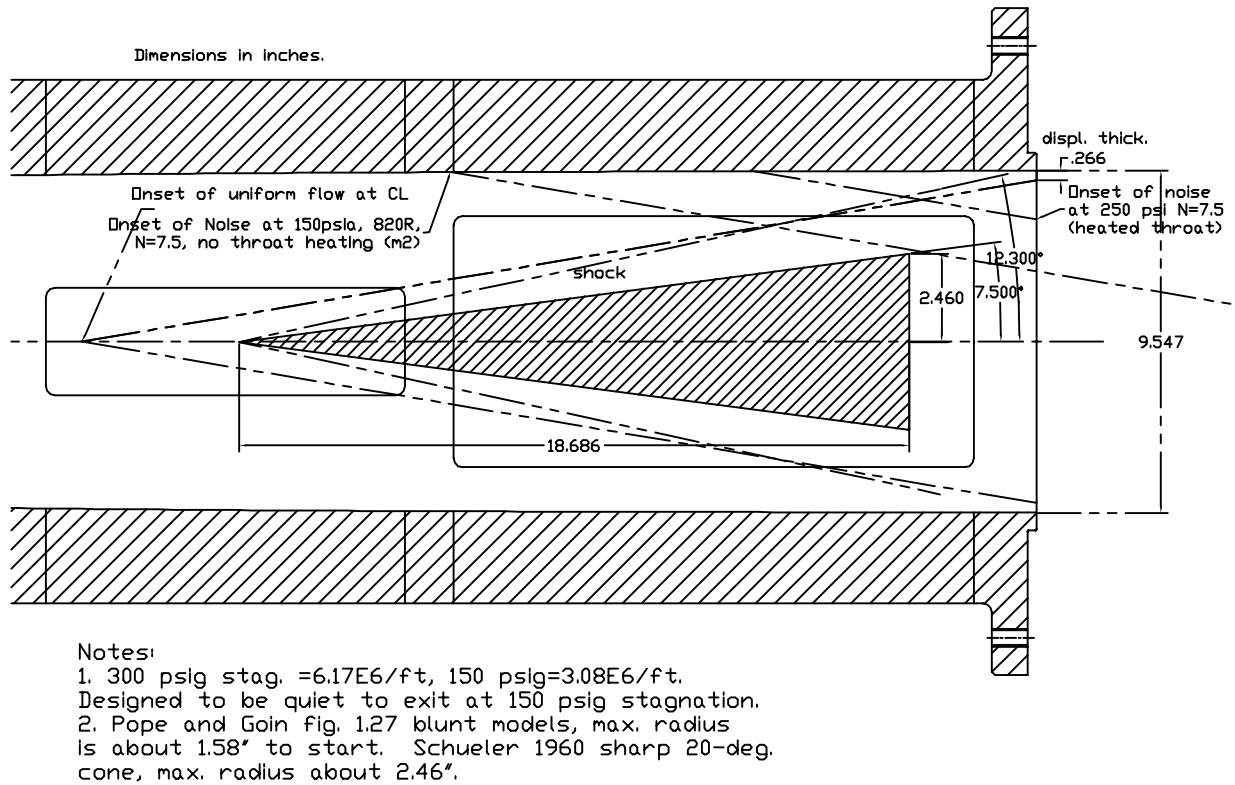


Figure 2: Schematic of Mach-6 Quiet Nozzle with Model

Roughness in Quiet-Flow Wind Tunnels

Creel et al. ca. 1986, LaRC Mach 3.5 Blocks

Creel et al. [17] looked at roughness and particulate effects in the Langley Mach 3.5 quiet-flow tunnel, which has 2D nozzle blocks. The original finish degraded due to insufficient air filtering, and was repolished. Measurements were made before and after repolishing, with a stylus instrument having a 0.0001 inch radius. Before polishing, the rms roughness was about 3-10 microinches rms, with local regions having rms roughnesses as large as 25 microinches. The peak-to-valley excursions were typically 15-50 microinches, with the maxima being about 55-100 microinches. After polishing, the rms roughnesses were reduced to 1-4 microinches, with local regions of 5 microinches rms. The peak to valley excursions were then 8-15 microinches rms, with maxima of 15-40 microinches. The table is also in Ref. [7].

Measurements were made of the transition Reynolds number on a round cone in the 'quiet flow' region, at various unit Reynolds numbers. Below 8×10^5 per inch, the results are the same for the two polishes. This corresponds to a throat unit Reynolds number of about 80 million per meter, and a stagna-

tion pressure of about 80 psia at 300K. At 1×10^6 per inch, the quiet Reynolds number increased from 4.5 million to 8.0 million with the polishing. This corresponds to a stagnation pressure of about 100 psia, and a throat unit Reynolds number of about 100 million per meter. Above this higher pressure the quiet flow performance degraded, presumably due to polish limitations.

These same data are summarized in Ref. [5]. Page 228 tabulates the data, reproduced here as Table 1. Here, values of the roughness Reynolds number are given for a Mach 3.5 unit Reynolds number of 42 million per meter, or about 105 psia at a guessed stagnation temperature of 300K, and a throat unit Reynolds number of 106 million per meter.

With the better polish, the higher throat unit Reynolds number is above the design conditions for the Purdue Mach 6, suggesting that if we match this polish we can probably meet the design. The lesser polish degrades the maximum throat Reynolds number by 20%, and thus degrades the quiet performance by roughly 20%.

Polishing/Plating of Mach 5
and Mach 6 Quiet Nozzles

	Avg. k for 5 locations				
	peak-to-valley				
Repolish	rms	typical	maximum	max local k	max R_k
before	3.9	24.0	72.0	100	42
after	1.7	11.6	22.0	40	12

Table 1: Roughness on LaRC M3.5 blocks; all values of k in microinches

Reference [38] describes experience with plating the Mach 5 quiet nozzle, which was made of electroformed nickel. The purpose was to try to improve surface hardness and resistance to oxidation. The attempt at plating hard nickel-phosphorous suffered from an error in electrode positioning which left unremovable pits near the throat.

Reference [39] describes similar experience with plating the Mach 6 electroformed quiet nozzle. The plating process was again flawed, but polishing techniques were developed which recovered part of the original nozzle performance. The plating process also left large nodules on the bleed lip.

The Mach-6 nozzle was honed, measured, and returned to Langley for testing. At this time, some profilometer measurements showed waviness of 0.0002 inch/inch or less (Fig. 4 in Ref. [39]). However, waviness of about 40 microinches over 0.040 inches existed still (page 7 and Fig. 3 in Ref. [39]); this is a waviness of 0.001 inch/inch. Table 1 in Ref. [39] reports that some waviness of 0.002 inch/inch existed at this time. Peak-to-peak roughness was as large as 32 microinches [39, Fig. 4c], and the rms roughness appears to have been about 4 μ in. Ref. [39] reports that ‘the performance of the nozzle was not satisfactory due to the waves.’ According to Steve Wilkinson (private communication, 31 Aug. 1998), he returned the nozzle after a visual inspection showed large waviness. The nozzle was therefore polished again, and returned to Langley.

These reports highlight the risks and difficulties in plating the electroformed nickel. They also show the extreme difficulty of removing pits. It is obvious that the excellent initial performance of this nozzle (good to 233 psia, 450K, and a throat Re of 1.4×10^8 per inch) requires extraordinary polishes that will be very difficult to maintain [63, 16, 10]. Pages 11 and 12 of Ref. [63] discuss the problem in detail.

Waviness Effects in Quiet-Flow Wind Tunnels

Beckwith’s Criterion for the Langley Nozzles

Ref. [9] shows results on the 2D Langley Mach 3.5 nozzle blocks that led to the criterion used by

Beckwith for waviness tolerances. Fig. 4 there shows waviness of 0.002 inch/inch which led to a Mach number variation of 0.045/inch on the centerplane. For an already-transitional boundary layer, an increase in noise was measured on the tunnel centerline at locations downstream of the waviness. This additional noise is believed to be due to the ‘shimmering’ effect of passing turbulence over the waviness. It is important to note, however, that there is no evidence that this 0.002 inch/inch waviness (with contour flaws of 0.002 inches and more) led to early transition [9, p. 4].

This difficulty with waviness led to a search for a better specification. Beckwith used Ref. [18], which reports measurements in the 50-inch diameter Mach-8 axisymmetric nozzle at AEDC (Tunnel B). Fig. 4 there shows waviness of 0.003 inch/inch which led to centerline Mach number disturbances of 0.01 per inch – the Mach number varied from 7.9 to 8.1 along the centerline. This deviation decreased to zero at a radius 2 inches from the centerline of the 50-inch diam. tunnel. The thick boundary layer on the tunnel wall did *not* smooth out the effect of the wall waviness. The nozzle was remachined to a waviness slope of 0.00036 inch/inch, after which the Mach number variation was reduced by a factor of roughly 4, so it is not particularly noticeable. This data led to Beckwith’s specification of a waviness tolerance of 0.0002 inch/inch (evident in Beckwith’s notes on the figure, and discussed privately in June 1991). Unfortunately, this specification is, at best, extremely difficult to meet.

Additional Langley experience can be found in Ref. [6], which discussed the shimmering effect of wall waviness on already transitional boundary layers. It cites Ref. [2], which shows data in two axisymmetric Mach-5 nozzles, one machined in sections and one electroformed. Fig. 12 in Ref. [2] shows the errors in the fabricated radius as a function of streamwise distance. The original machined joint had a backward-facing step of about 0.004 inches, and did not have any quiet flow. It was remachined to have a waviness of 0.006 inch/inch near the throat, with a peak deviation of 0.006 inches, after

which it still did not have any quiet flow. The waviness in the electroformed nozzle was lower, with a peak of about 0.004 inch/inch that had a greatly decreased peak deviation of 0.0006 inches. The electroformed nozzle was quiet at low Reynolds numbers.

Waviness Effects on Centerline Mach Number

A number of other papers discuss the effects of wall waviness on the uniformity of centerline Mach number in axisymmetric nozzles, pointing out the difficulties with wave focusing there.

Korte et al carried out PNS computations for the effect of wall waviness in the Mach-8 quiet tunnel on the centerline uniformity (Wilkinson, private communication, March 1996). A 0.001 inch/inch wave placed at $x = 5.8$ inches caused a Mach number deviation of 0.005 near the exit.

Midden reports measurements of centerline focusing in the Langley Mach 6 CF_4 tunnel [30]. Pitot pressures at the nozzle exit showed a perturbation of 20-30% peak-to-peak, apparently due to a flaw in the nozzle contour. These fluctuations caused substantial variations in pitot pressure on a 4-inch diameter hemisphere, when the hemisphere was placed on centerline near the perturbation. Unfortunately no measurements of the nozzle contour are reported.

Micol reports measurements of a remachined nozzle in the same wind tunnel [29]. They state that the centerline disturbance mentioned above was only visible for stagnation pressures of 1000 psia or above. They also suggest that the disturbance may in part have been due to flaws in the nozzle design procedure. The new nozzle was machined to a tolerance of 0.0005 inches in the throat, and 0.001 and 0.002 inches farther downstream. Measurements show that large perturbations in the mean flow are no longer present. This work is also discussed in Ref. [28]. Micol reports (private communication, April 1998) that the wall contour data do exist but are unpublished.

Additional measurements of flow quality in a Mach-6 nozzle are reported in Ref. [14], and related to measurements of the wall contour. Ref. [12] shows related flow measurements in the same nozzle, but does not include the wall deviation measurements.

Summary of Roughness and Waviness Effects

No systematic study of these effects has ever been carried out, so the data is incomplete and ambiguous. Nevertheless, tolerances and specifications must be provided to fabricators.

The following preliminary conclusions are therefore offered:

1. The Purdue nozzle specifies an allowable peak roughness based on the $Re_k = 12$ criterion. A factor of 30 was used to relate peak roughness to rms roughness; this factor, obtained from I. E. Beckwith, is probably generous. The criterion is only a guide, and the best polish affordable should be obtained near the throat. Since the largest flaw cannot be found with standard inspection methods, nothing further can really be done with this issue. Extreme care is being taken to keep the airflow clean, so the polish does not degrade; limitations in the air cleanliness, the original polish, and the nozzle hardness will be key issues in overall nozzle performance.
2. It seems that waviness causes problems due to slope and amplitude combined. Slopes of 0.001 inch/inch or larger cause variations in the mean flow. Slopes of 0.001 inch/inch or larger, when combined with peak deviations of 0.001 inch or larger, can cause larger mean flow effects or even trip the flow. Thus, the waviness specification should be considered in conjunction with the accuracy specification.

MEASUREMENTS ON THE TEST JOINT

The nozzle must be built in sections. The upstream sections are machined, then the next downstream section is attached, and a final machining is done, feathering over the joint. A test joint was built to determine how accurately this could be done (see Fig. 3 and Ref. [46]). There are two joints in such a machining: the physical joint between the two parts, and the joint where the two separate machinings are matched up. Between the two machinings, the part has to be removed from the lathe for assembly, and then realigned. This critical realignment process must be carried out with great precision, to meet the required tolerances. Maintenance of a smooth finish at the physical joint is also an issue. The Langley Mach-8 nozzle had some joints which initially appeared smooth, but in which visible steps appeared after some cycles of heating and cooling (Steve Wilkinson, private communication). The Langley Mach-8 also has had problems with leaks at the joints. Lessons learned from this Langley experience were incorporated into the design of the present joints, which are far more robust.

The smaller end of the test joint was finish-machined, and polished to a mirror finish (simulating the effort that would be needed on a multi-section polished nozzle). It was then assembled to

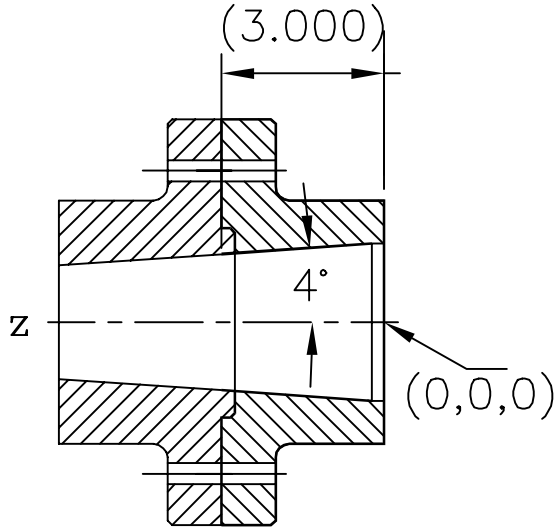


Figure 3: Schematic of Test Joint: Dimension in Inches

the larger end, finish-machined, and measured at DEI. For the first cut of the test joint, a 0.003-in. step appeared at the line between the two separate machinings, as shown in Figure 4. Here, z is the coordinate along the axis of the part, while x and y are coordinates in the radial direction. Measurements were taken along four rays at 90-deg. azimuthal angles. Fig. 4 shows the deviations (Δx and Δy) between the measured and nominal coordinates. The radius is about 0.002 inches too large on the narrow end, and about 0.001 to 0.002 inches too small on the wide end. Although no step appears at the mechanical joint (at $z = -2.75$ in.), the step or wave at the blend between the two machinings is far out of tolerance. This wave, at $z = -3.5$ inches, has a slope of about 0.0034 inch/inch.

The test joint was then heated in an oven at DEI (to roughly 550F), allowed to cool, and measured. This cycle was twice repeated, to see if any steps appeared near the mechanical joint. The results are shown in Fig. 5. Measurements are shown along two rays, at 180-deg. intervals in azimuth. The step or wave shown in Fig. 4 is of course still present. The measurements for heat 1 are shifted slightly upwards, probably due to a misalignment of the part in the measuring apparatus. Otherwise, it is evident that all 3 measurements are nearly identical, and that no step develops at the mechanical joint. The test joint was later heated to about 450F in an oven at Purdue, placed in a lathe, and measured while hot with an 0.0001-inch dial indicator. No step could be detected at the joint. The resolu-

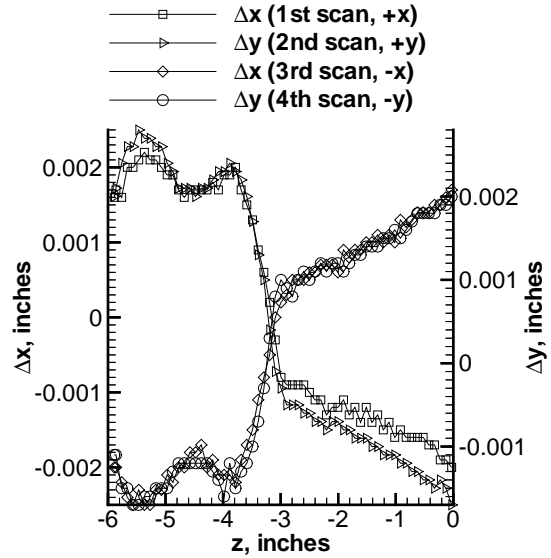


Figure 4: Test-Joint Contour Errors After First Cut

tion of this measurement was roughly 0.0001 inches.

After the above measurements, the test joint was shipped back to Optical Technologies (Franklin Park, IL) for final polishing. Optical Technologies worked primarily on the region near the joint, and did not polish near the large end. The part was then sent to NASA Langley for measurement in a Rank-Taylor-Hobson Talysurf profilometer, by Kenneth Hall [48]. The stylus radius was 2μ , or $79 \mu\text{in}$. An unpolished part of the inside diameter is shown in Figure 6. In Figs. 6 to 8, x is a coordinate along the surface, and z is the height of the surface. The regular waviness is consistently observed, and appears to be the toolmarks from the lathe-turned part. The peak-valley height is about $120 \mu\text{in}$. There is a small long-wavelength alignment error, which is ignored when considering roughness. As measurements were made closer to the joint, this waviness slowly decreases. Figure 7 shows typical results from a semi-polished region. Finally, in the joint region the finish is very good, as shown in Figure 8. It is evident that the polisher was able to achieve an excellent finish without removing more than about $120 \mu\text{in}$ of stock. This is critical, for three reasons. First, the small amount of material removed means that the contour accuracy and waviness achieved in the machining or grinding process can be maintained in the hand polishing process. Second, the high polish achieved may enable quiet nozzle operation at significantly higher unit Reynolds numbers. Third, the peak-valley roughness is only about 6 times the

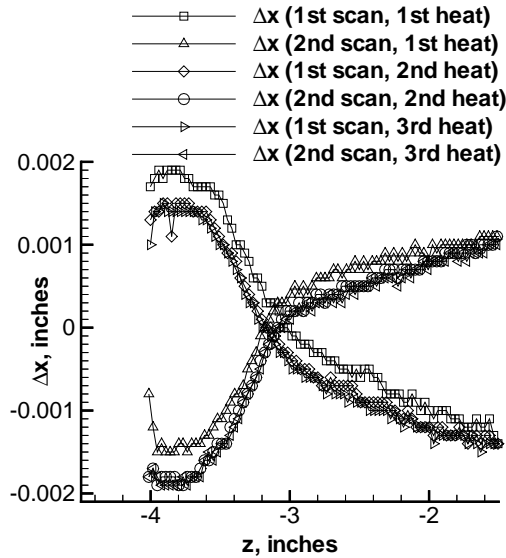


Figure 5: Test-Joint Contour Errors After Thermal Cycling, First Cut

RMS, a value much lower than the 30 times usually assumed by Beckwith. However, these peak-valley measurements were only obtained along a line, and do not represent the largest roughness in the whole area, which is the critical issue for quiet flow.

The test joint was then used one more time, to determine whether it was possible to blend the two separate machining processes without introducing the large wave seen in Fig. 4. Great care was taken in the development of the process for realigning the part in the nozzle (normally carried out after assembly of the two sides). Although the two sides were not re-separated for this test, the part was removed from the lathe after machining the contour in the small end. The part was then set up in the 4-jaw chuck again. A number of surfaces were added to allow precision indication of the part location (see Ref. [26] for details of the fabrication process).

Figure 9 shows the resulting measurements. Again, these were taken on 4 rays at 90-deg. azimuthal intervals. Scan 1 measures positive x, 2 measures positive y, 3 is negative x, and 4 is negative y. The taper is evident. The last section near $z=0$ was made flat on purpose, as part of the multi-section alignment and blending process.

Figure 10 shows the deviation of the measured coordinates from the nominal coordinates. Even near the blend location, no step or wave is apparent. The positive x and y deviations increase with decreasing z, while the negative ones scatter around

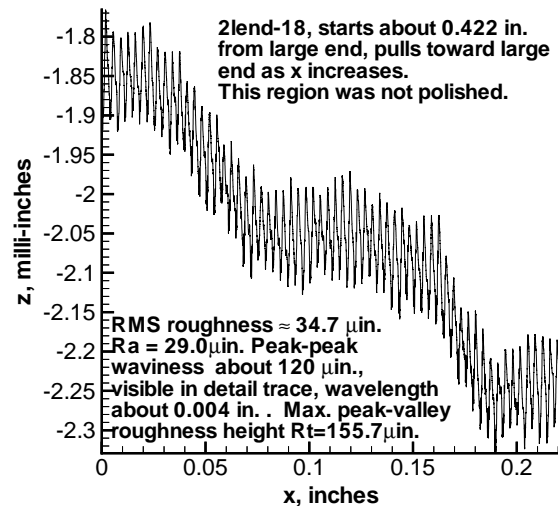


Figure 6: Test-Joint Roughness: Unpolished Region

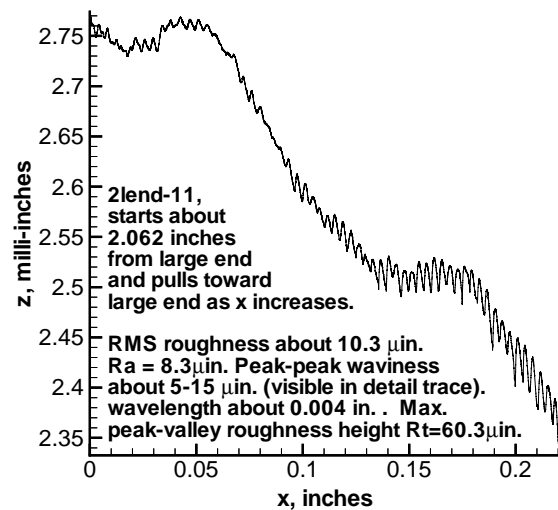


Figure 7: Test-Joint Roughness: Semi-Polished Region

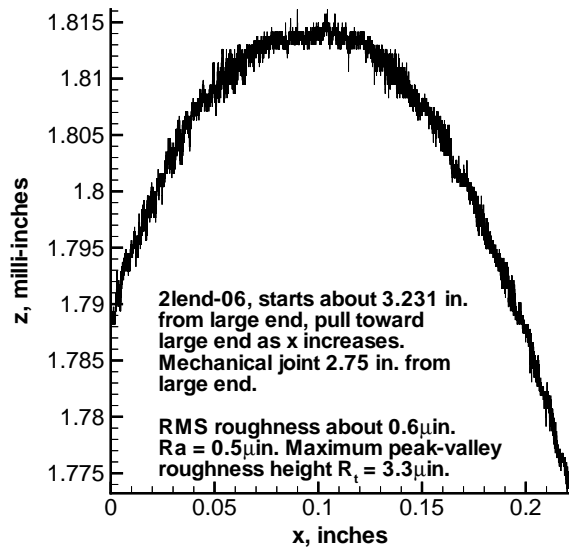


Figure 8: Test-Joint Roughness: Highly Polished Region

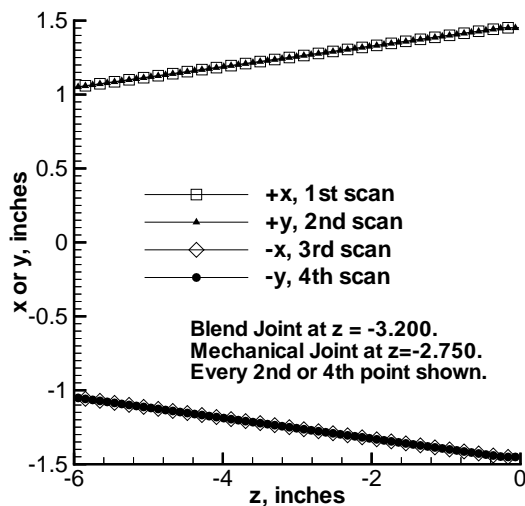


Figure 9: Test-Joint Recut: Measured Contour

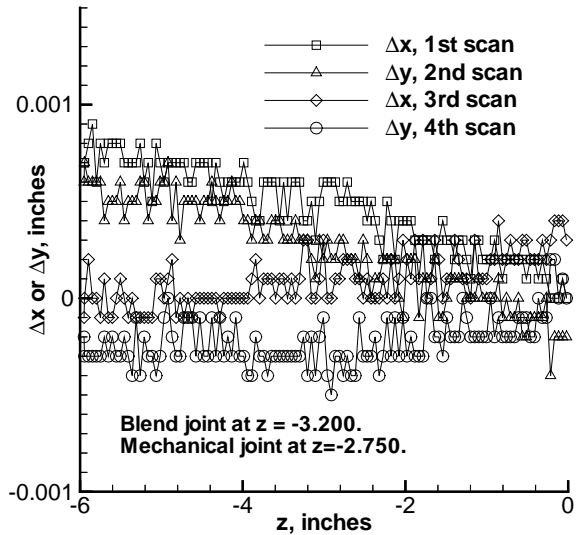


Figure 10: Test-Joint Recut: Deviations from Nominal Contour

zero. An radial flaw of $0.0008/2$ in 6 inches corresponds to an angular error of about 0.004 degrees. Since the small end is a bit large, this is 0.004 degrees below the nominal 4.000 deg., or 3.996 deg. This slowly tapering error will have no real effect in the nozzle, presuming that all the joints can still be made smooth.

The waviness was computed for each scan, using a method that originated with Steve Wilkinson at NASA Langley. The waviness is computed as a linear fit to 11 points spaced at about 0.049 inches. The results are shown in Figure 11. The waviness is within ± 0.0006 inch/inch throughout. This is a 6-fold improvement on the blend-flaw in the original cut.

The test-joint effort was thus successful in developing and proving the manufacturing processes, at minimal cost. A joint of sufficient smoothness can be fabricated and maintained smooth even under thermal cycling. This machined surface can be polished by removing small amounts of material (less than 0.0005 inches), thus maintaining the machined waviness. The process of blending joints between machinings of separate sections can be accomplished with excellent accuracy, given sufficient care. These successes enabled nozzle fabrication to begin, with good confidence.

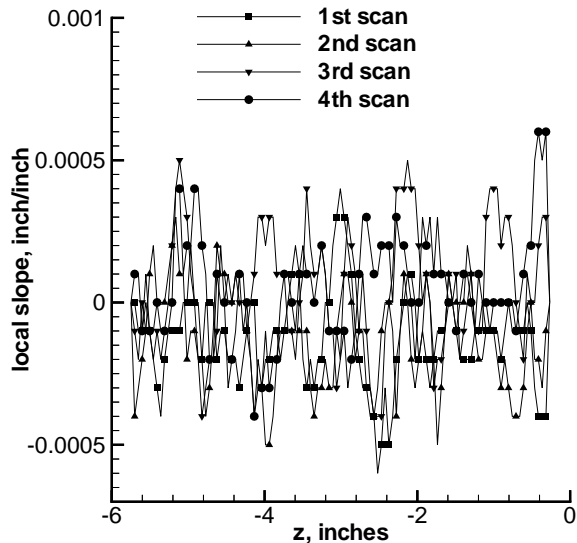


Figure 11: Test-Joint Recut: Waviness

NOZZLE THROAT ASSEMBLY WITH ELECTROFORMED NOZZLE

Introduction

Despite the success of the test joint recut, concern about steps at the nozzle joints remained. The critical throat region has extremely tight roughness tolerances [47, pp. 28-29]. The allowable peak roughness rises to 0.001 inches only at 9.3 inches downstream of the throat. To accurately machine the internal contour in a lathe, the section lengths must be limited, so that the boring bar is not too long, and does not chatter or deflect too much. A nozzle built completely by turning on a lathe was drawn, requiring section joints that were 3.76 and 9.01 inches downstream of the throat. At 3.76 inches, the maximum allowable peak roughness is about 0.00036 inches. To reliably achieve this smoothness at a joint appeared to be a major risk. Thus, it was decided to electroform the throat section of the nozzle, thereby combining the electroform approach of the Langley Mach-6 nozzle with the machined-section approach of the Langley Mach 8.

Figure 12 shows the throat-region assembly with the electroformed sleeve. The first joint seen by the flow is located about 19.3 inches from the throat, where the allowable peak roughness is about 0.0029 inches. Using Beckwith's criterion where the RMS should be about 1/30 of the peak, the RMS roughness downstream of this joint should be less than 100

μin . This is easily met with an off-the-lathe finish of 16-32 μin . The unusual surface finish requirements are thus limited to the electroformed section. This is formed all in one piece on a single mandrel which can be ground and polished externally, with ease, since the electroform is supposed to reproduce the finish of the mandrel.

Test Mandrel and Electroformed Nickel Issues

The electroforming of the throat section then became a critical issue. Although electroforming was used successfully for the LaRC Mach-6 quiet-flow nozzle [16, 10], the initial performance of the LaRC Mach-6 apparently degraded after initial operation. A possible cause was surface degradation in the throat, associated with hot operation. However, the initial data is not conclusive, according to Steve Wilkinson, and so the true cause of the apparent degradation is unknown.

Low-cost and simple tests of this hot-operation degradation were desirable, in order to reduce risk. In addition, the Purdue nozzle is to introduce the use of a hard layer of electroformed nickel, approximately 1/8-inch thick, on the surface near the flow. Both the hard and soft nickel are nearly pure, and are prepared from a sulfamate bath by GAR Electroforming, Danbury CT, the same vendor used for the LaRC Mach-6 nozzle. The hard nickel bath differs only by the addition of trace amounts of saccharin. This hard nickel, Rockwell C33-38, should be much more scratch-resistant than the soft nickel used in the LaRC nozzle (Rc 21-23). However, this also introduces concerns about cracking, delamination, or other problems with the hard nickel.

References [41] and [25] are some recent reviews of electroforming. The material hardness, strength, ductility, and so on are strongly affected by the process used. Impact resistance tends to decrease with increasing hardness. Corrosion was also a concern, since Frank Chen (NASA Langley, private communication) thought it might be the cause of the degradation in the performance of the NASA Langley Mach-6 nozzle. According to Ref. [19, p. 42], '*Although some tarnishing may occur, nickel has extremely low corrosion rates in strictly marine and rural atmospheres*'. Below 400C, corrosion should be negligible (see Ref. [19] and references cited therein), so any corrosion would be unexpected.

Electroformed-Nickel Test Samples

To reduce risk, tests were carried out on samples of the hard and soft nickel that were procured from GAR. These 2 by 2-inch samples were plated

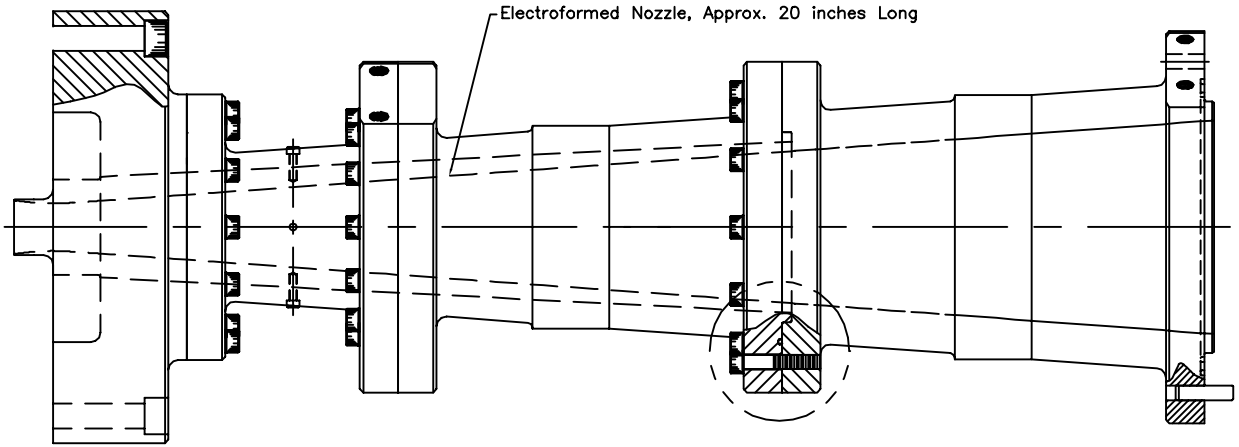


Figure 12: Electroformed Throat Assembly, 1/5 Scale

onto glass or aluminum plate substrates, and then removed by GAR. The details are described in Ref. [52] and [51]. The surface finish of the first soft nickel sample became cloudy after first being heated. However, this was apparently due to residual effects of the surface preparation used by GAR in the initial electroforming, for the problem did not repeat, after a light polish and a second heating. The hard nickel coupon did not degrade visibly after 24 hours at 422F, even on first heating.

Both coupons were measured in a Zygo interferometric profilometer, by Chris Tieche at Purdue. Several images were taken of each coupon; the Zygo computes RMS and peak-valley maximum roughnesses from the roughness-height image. The RMS surface roughness of the hard coupon was 7-57 nm or 0.3-2.2 $\mu\text{in.}$ The larger value only occurred on the occasional samples in which large pits were detected. These pits were roughly 10 μ (400 $\mu\text{in.}$) wide and 1 μ (40 $\mu\text{in.}$) deep. The soft nickel coupon had an RMS roughness about half this, with similar occasional pits. It appears that the electroforming will generate occasional pits, which hopefully will not act as boundary-layer trips. The hard nickel coupon also contained some cracks around the edges (only), which again raised concerns about ductility. It was also apparent from this series of tests that a proper simulation of the nickel electroform required deposition onto a substrate that is similar to the actual nozzle mandrel.

The actual nozzle electroform is to contain a combination of hard and soft nickel in layers: the first layer near the inside surface is to be about 0.12-inch thick. Hard nickel is not to be used throughout, due to difficulty in machining the outside diameter, and to the additional expense. This raised concerns

about possible debonding at the joint. Such debonding might be caused if the inner nickel layer had a smaller thermal expansion coefficient than the outer layer. While a thermal expansion coefficient was available for the soft nickel, none was reported by GAR for the hard nickel. To test these concerns, a layered nickel specimen was obtained from GAR. The 6 by 6 inch sample was roughly 3/8-inch thick, with equal layers of soft and hard nickel. Unfortunately, the sample separated from the conducting plate during electroforming, and the surface was deformed. The sample was ground mostly flat, except for some low points, after which it was about 17/64 inch thick. It was flat to about 0.002 inches over the 6-inch length, as measured using a dial indicator and a surface plate. The sample was then placed in an oven at 423F for 5 hours. Measured hot, it remained flat to within about 0.002 inches. The lack of curling can be analyzed to infer that the thermal expansion coefficients remain within about 2% of each other. Concerns about debonding were relieved.

The ductility concerns were addressed by carrying out plane-strain fracture toughness tests. These provide a simple approximate assessment of the brittleness of the specimens. Although the available specimens were too small to achieve a valid benchmark plane-strain fracture toughness per ASTM E399, the results were still useful for comparative purposes. These tests were carried out by Mr. Jason Scheuring, a graduate student under the supervision of Prof. Grandt. The results are shown in Table 2. Here, W is the sample thickness, in inches; all specimens were 1.8 by 1.875 inches in planform. Also, N is the number of specimens tested, and Kc is the fracture toughness, in ksi- $\sqrt{\text{inch}}$. The aluminum specimen was tested to have a benchmark with a

Mat'l	N	W	Kc
6061T651 alum.	2	0.25	30-34
layered Nickel	3	0.26	27-28
soft Nickel	1	0.2	38
hard Nickel	1	0.14	100

Table 2: Plane-Strain Fracture Toughness of Samples

commonly accepted material.

Conclusive results were not obtained, since the fracture toughness Kc increases with decreasing thickness in a manner which is unknown. However, the high value for the (thinner) hard nickel specimen suggests that the hard nickel is at least as tough as the softer nickel or the aluminum. Certainly the hard nickel is not extremely brittle like glass. Concerns about ductility were relieved.

Test Mandrel and Test Electroform

To further reduce risk in the polishing and electroforming process, it seemed desirable to carry through the complete process using a small test mandrel. This mandrel is shown in Fig. 13. The mandrel is made of Optimax stainless steel. The final machining was carried out at Purdue after heat treating to Rockwell C43-47. No grinding step was included. The tapered surface was then polished by Optical Technologies to a sub-1-micron finish. Optimax is a 420 stainless steel that is available from Uddeholm Inc., of Sweden. It is specially made to be highly polishable with excellent microcleanliness. It is said to undergo three vacuum remeltings in a clean room. Paul Thomas of Optical Technologies has had excellent experience using it for highly-polished CD-ROM molds.

The test mandrel was then measured in the Zygo interferometer at Purdue, by Chris Tieche [56]. While this will not be possible for the large nozzle-throat mandrel, it was another good opportunity to measure the sample finish produced by Optical Technologies using the same processes. Ten sample areas were measured, each an 0.08 mm square. The RMS roughnesses measured were 8-18 nm, or 0.3-0.7 $\mu\text{in.}$ The peak-valley excursions were generally around 500 nm, or 20 $\mu\text{in.}$ Here, the peak/RMS ratio is more similar to Beckwith's estimate of 30. Areas 9 and 10 had protrusions with heights of about 300 nm, although these were thought to be dust specks. Area 8 had 4 pits, which were the only large defects Chris believed were actually in the material. These pits were roughly 500 nm deep (20 $\mu\text{in.}$) and

5 μ wide (200 $\mu\text{in.}$). The mandrel surface finish appeared to be excellent, despite the presence of these few small pits.

The mandrel was then electroformed at GAR. The 1/4-inch thick electroform was composed of an inner layer layer of hard nickel and an outer layer of soft nickel, each 1/8-inch thick. The electroformed mandrel was returned to Purdue. Flats were machined on the outside diameter (o.d.) of both ends. The nickel overhanging the large end of the mandrel was then machined off, to allow removal. Unfortunately, the electroform broke free during the machining. Apparently, small mandrels break free much more easily than large ones do. The inside surface appeared excellent, except for some scratches near one end which probably occurred when chips entered the gap after the electroform broke free on the lathe. The mandrel was then cut in two halves, to form two hollow cones.

The larger (round) section was then placed in an oven at 197C (387F) for 24 hours. It had a mirror surface after removal from the mandrel, and cleaning with acetone; this mirror surface remained after the heating, with no apparent change. The o.d. of the large end before heating was 2.1983-2.1990 in. When hot, the o.d. ranged from 2.2013 to 2.2020. The o.d. of the flat on the other end was 2.0805-2.0818 before heating. When hot, it was 2.0838-2.0848. The electroform appeared to expand uniformly with no visible problems, with an expansion of about 0.0015 inch/inch at approx. 300-400F. GAR quotes 7.5×10^{-6} in/in-F for the thermal expansion coeff. for the soft nickel. 300F would correspond to 0.0023 inch/inch. 0.0015 inch/inch corresponds to 200F; it is possible that the sample cooled this far while being measured. The test mandrel electroform thus appeared well behaved.

The smaller round section was then cut lengthwise into halves, using a slitting saw. One half was then further cut into quarters. These arc sections allowed measurements to be carried out on the inside diameter (i.d.) using the Zygo (a process that will not be possible with the actual mandrel). Measurements on the two quarter sections were first carried out, before heating [54]. No defects were visible to the naked eye, according to Chris Tieche, so the ten Zygo images obtained for each specimen are random samples.

Most of the sample areas showed excellent finishes, about 10-15 nm RMS (0.4-0.6 $\mu\text{in.}$), with peak-valley variations of roughly 200 nm (8 $\mu\text{in.}$) However, several areas showed pits, with depths of roughly 200 nm and widths of roughly 5-10 μ (200-

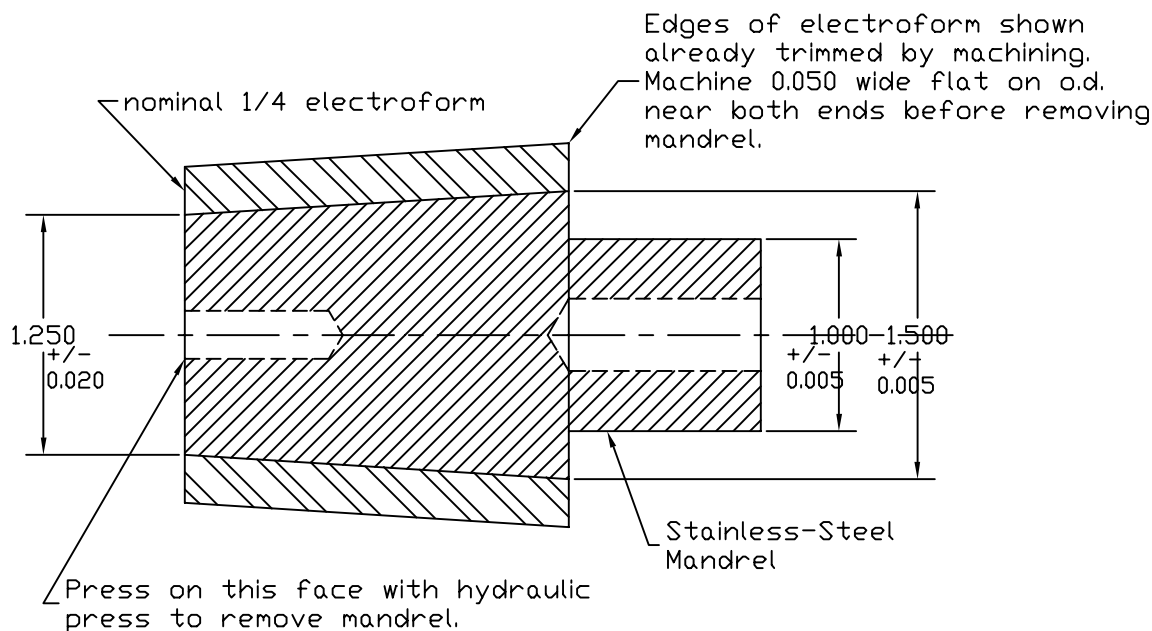


Figure 13: Section Drawing of Test Mandrel for Electroforming. Full Scale. Dimensions in Inches

400 $\mu\text{in.}$) Area 2 of specimen 2 showed a large peak, with a height of about 1300 nm (51 $\mu\text{in.}$) and a width of about 5 μ (200 $\mu\text{in.}$) Figure 14 shows the Zygo contour plot, although much is lost in the translation to gray scale. The horizontal bar is where the line profile of Fig. 15 is taken from.

Area 4 of specimen 2 exhibits a ridge of roughly 50 μ (0.002 in.) length and 0.5 μ (20 $\mu\text{in.}$) height, and some of the other areas also have significant roughness. The electroform has defects of up to 50 $\mu\text{in.}$ peak, which is marginally within spec. The Purdue Mach-6 quiet nozzle specification calls for 91 $\mu\text{in.}$ peak flaws in the throat region, according to Beckwith's $Re_k = 12$ criterion [47], at the nominal operating pressure of 10 bar. It may be desirable to polish the electroform after assembly. It is not clear how these results relate to Langley's, which were mostly obtained with profilometers. These do not identify the peak roughnesses as well.

After these measurements, the electroform test specimens were placed in an oven at 197C (385F) for 67 hours. It was then remeasured in the Zygo [53]. Longitudinal ridges were noticed, for the first time. Typical results are shown in Figs. 16 and 17, for area 3 of sample 1. Note that the peak to valley roughness of these ridges is about 50 nm (2 $\mu\text{in.}$), so these are fairly small. While this roughness appears to be somewhat changed from the preheating measurements, it is still small. However, area 2 of specimen 2 showed a 15 $\mu\text{in.}$ deep pit, and area 3

of specimen 2 shows a 20 $\mu\text{in.}$ peak about 400 $\mu\text{in.}$ wide.

These larger roughnesses are comparable to the preheat results. It may be that the peaks correspond to pits similar to those observed in the test mandrel. Large flaws in the electroform seem more common, so it also seems possible that some develop in the process. The results are within the specification, but not as good as was hoped for. It may be desirable to polish the actual nozzle throat after initial operation, to see if this polish can improve performance. The hard nickel to be used should aid this polishing process.

Nozzle Throat-Region Mandrel No. 1

The mandrel and the throat-region electroform are on the critical scheduling path, since the other nozzle sections cannot be completed until they can be faired to a completed throat. The first mandrel for the throat-region electroform was built out of Optimax stainless steel, heat-treated by Uddeholm to Rc43-47. The material was ordered on contract initiation in Jan. 1999; delivery of this large piece of specialized material took about two months. The mandrel was rough-machined at DEI and ground at D.M.C. International, Harrison Township, Michigan. In May 1999 the contour of the ground mandrel was measured at DEI. The first set of measurements was compared against a nominal contour that was interpolated from the original design data with in-

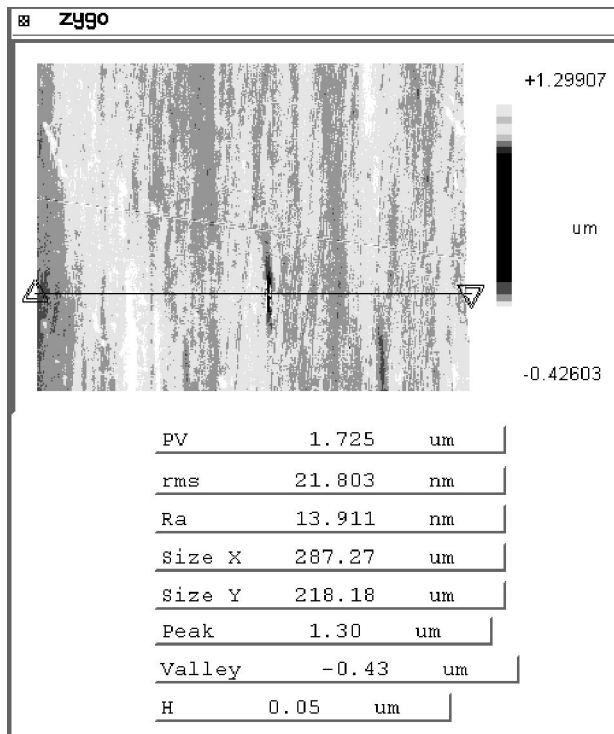


Figure 14: Largest Surface Roughness in Specimen 2: Grayscale Version of Color Contour Plot

sufficient accuracy. The original measurements were then compared against an accurately interpolated nominal contour. The measurements were made along four rays at 90-deg. azimuthal angles; the measurements along the 0-deg. ray are typical, and are shown in Fig. 18. Here, z_1 is an axial coordinate on the centerline, with arbitrary axial origin. The deviation from the nominal contour is within ± 0.0005 in., an excellent result. Figure 19 shows the waviness, computed using the same 11-pt. fit from measurements that are again at intervals of about 0.050 in. The waviness is within ± 0.0005 in./in., again an excellent result.

The mandrel was then polished by Optical Technologies. Unfortunately, initial polishing revealed pits that occurred randomly throughout the mandrel surface. The part was then inspected by Tom Hillskog, a Uddeholm metallurgist. His tests on a sample taken from the arbor did not show any reason for the pitting. Following his suggestion, further material was stoned from the mandrel, since the mandrel was useless in the pitted form anyway. An excellent finish was then obtained.

Since the amount of material removed was now a concern, the contour was remeasured at DEI, in August 1999. The contour measurements are shown

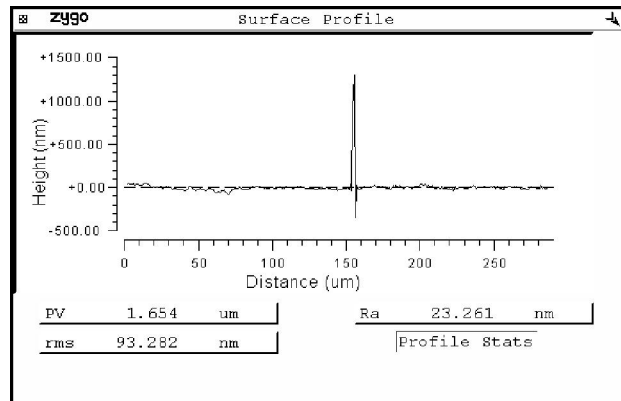


Figure 15: Profile of Large Roughness in Specimen 2

in Fig. 20. Here, z is an axial coordinate on the centerline, with $z = 0$ at the throat. Because of the hand polishing, measurements were made along 6 azimuthal rays at 60-deg. intervals. Along most of the mandrel, the radius was about 0.001 inch undersize, which should not cause large mean-flow deviations, so these data are not shown. However, there is a problem near the throat, as detailed in Fig. 21. Here, the error and the slope are shown for the rays with the biggest problem. The zero slope plotted near $z = -1$ is an artifact of the 11-point fitting scheme and should be ignored. It is evident that the extended polishing in the critical throat region removed about 0.004 to 0.006 inches of material, and did so nonuniformly, introducing waviness. The peak waviness is nearly 0.005 inch/inch, with a correspondingly large contour deviation of roughly 0.002 to 0.003 inches.

This waviness (or slope) is well outside the specifications. To reduce this waviness, efforts were made to redesign a new nominal contour with slight variations from the initial one, but none were successful. Due to the risk of nozzle-wall instability and transition that might be caused by the waviness, the part had to be rejected. The root problem was the extra material that had to be removed in order to eliminate the surface pitting.

A piece of the mandrel was then sent to Uddeholm for analysis, since Uddeholm warrants the polishability of Optimax. While it seemed strange that only the surface layer was pitted, it still seemed possible that a bad grain structure in the material could have developed small pits or tears in the grinding process. In Dec. 1999 Uddeholm informed us that *'The steel grade is Optimax as declared and we have confirmed the presence of coarse primary carbides.*

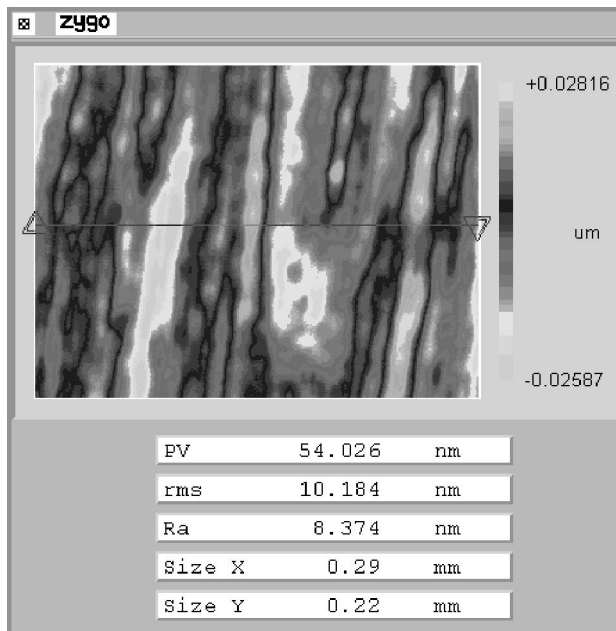


Figure 16: Typical Roughness after Heating: Grayscale Version of Color Contour Plot

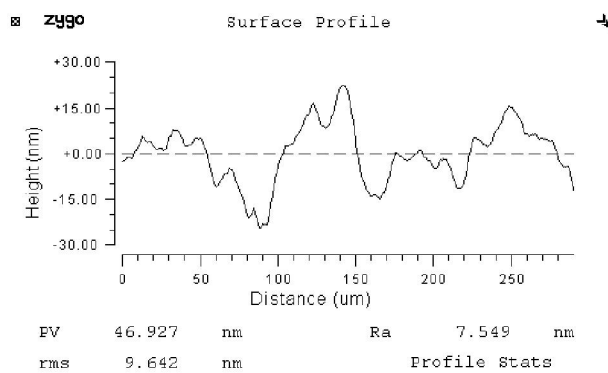


Figure 17: Profile of Typical Roughness after Heating

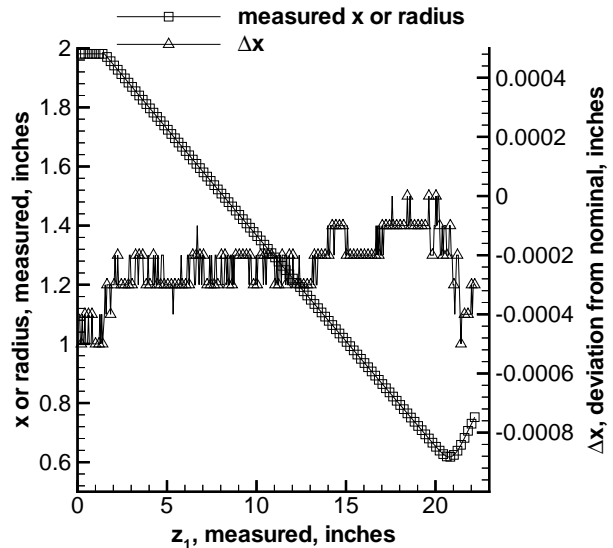


Figure 18: Contour and Error in Mandrel 1, Before Polishing

This fault appears in such a way, that it must have existed already in the bar as delivered. Consequently, the complaint is approved' [37].

Uddeholm (Tom Hillskog) states that this was an isolated problem with slow cooling in the heat treat, and should not repeat. In the meantime, the test mandrel (also Optimax) had been reground at DMC. Although scanning-electron-microscope images showed some peculiar surface voids [27], it was then repolished at Optical Technologies, with excellent results. Eight sample areas were measured in the Zygo interferometer, and showed RMS roughnesses of 0.3-0.5 $\mu\text{in.}$, with peak-valley variations of 4-8 $\mu\text{in.}$ [55]. Some pits with 3-6 $\mu\text{in.}$ depths were observed, but these are small. Thus, there appeared to be no systematic problems in the processes.

Nozzle Throat-Region Mandrel No. 2

Following the Aug. 1999 determination that Mandrel 1 had to be scrapped, material was ordered for a replacement mandrel. Since the cause of the failure of Mandrel 1 was at that time unknown, 15-5PH stainless steel was used instead, after ultrasonic inspection to Grade AAA. This is the same material that was used for the Langley Mach-6 quiet nozzle, except single vacuum remelt was used, since double vacuum remelt is no longer available. Extra material was obtained, so that part could be cut off to serve as a witness specimen. This witness specimen was examined under a 40-power binocular microscope in early October, and found to have scratches and pits.

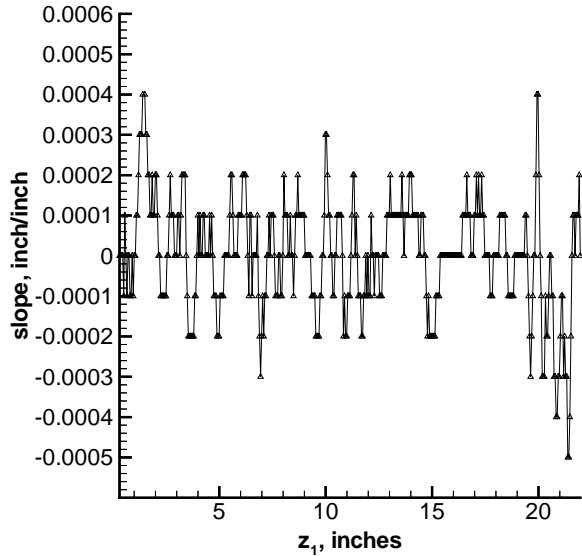


Figure 19: Waviness in Mandrel 1, Before Polishing

Optical Technologies then attempted to polish the specimen, but found that it would not take a good polish due to material defects. Optimax was then ordered for a third mandrel.

A new vendor for the grinding process had in the meantime been identified. Schmiede Corp. of Tullahoma, Tennessee also has experience with similar high-tolerance grinding, and the quoted price was an order of magnitude lower. The second mandrel was ground at Schmiede as a test of their processes. The contour accuracy was again excellent, as shown in Fig. 22. Figure 23 shows the waviness slope, which is well within the 0.001 inch/inch tolerance. The grinding appeared to be successful.

Despite the failure of the polishing attempt on the witness specimen, tests of the polishability were then carried out. The mandrel was first studied under the 40 power binocular microscope. A 0.040-in. diam. ballpen tip was used to estimate scale. Many azimuthal gouges were evident, especially near the throat, apparently from the grinding process. These appeared to be 0.004-0.010 in. wide and roughly 0.040 in. long. A number of pits and voids were also observed; these appeared to be inherent in the material. One of these looked like a rift in a muddy field, and was about 0.020-0.040 in. long and 0.010 in. deep [50]. A trial polish at Optical Technologies was unsuccessful. Paul Thomas believes that the grinding marks may have been due to bad carbides in the steel, which tend to tear upon the grinding wheel. He also noted that it is critical to keep a

Plots 1-6 are labeled A-F and correspond to measurements along 6 planes at 60-deg. azimuths. The throat is located at $z=0$, the bleed lip tip at $z=-0.97$, and the mandrel ends at about $z=19.25$.

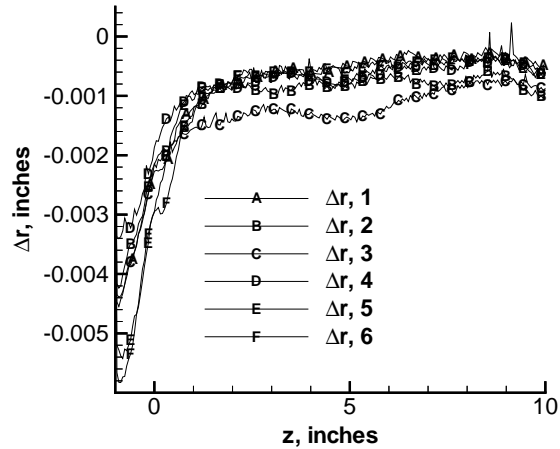


Figure 20: Contour Error in Mandrel 1, After Polishing

clean wheel, free of abrasive specks, which will otherwise cause grinding tears. Such tears cannot be removed in polishing, without excessive material removal that will cause waviness as with Mandrel 1. The use of a Borzon wheel was suggested, since this wheel embeds the abrasive in a rubbery wheel and it thought less likely to leave free abrasive specks.

Mandrel 2 was returned to Purdue for additional examination under the 40 power binocular microscope. The third (trinocular) head was now fitted with either a reticle or CCD camera [50]. The reticle has 100 divisions, each about 0.0005 inches, as calibrated with a machinist's scale. Defects were identified, measured with the reticle, and then imaged. Figure 24 shows some gouges; the near edge of the gouge is about 0.048 in. from the parting line, which can be seen near the right-hand side. The gouge oriented at about 45-deg. is about 0.0025 by 0.0075 inches. The depth appears to be about half the width. The parting line at the throat is about 0.0005 inches wide. This line cannot be made to completely disappear, which suggests that it may be necessary to polish the electroform. Figure 25 shows the largest gouge observed, about 0.075 inches long, visible to the naked eye, and located about 6 inches downstream of the throat. It is about 0.0025-0.003 inches wide, with a depth that appears to be about half the width. The rest of the surface is blank, as a good surface should be. Defects which scatter light differently and are so apparent to the

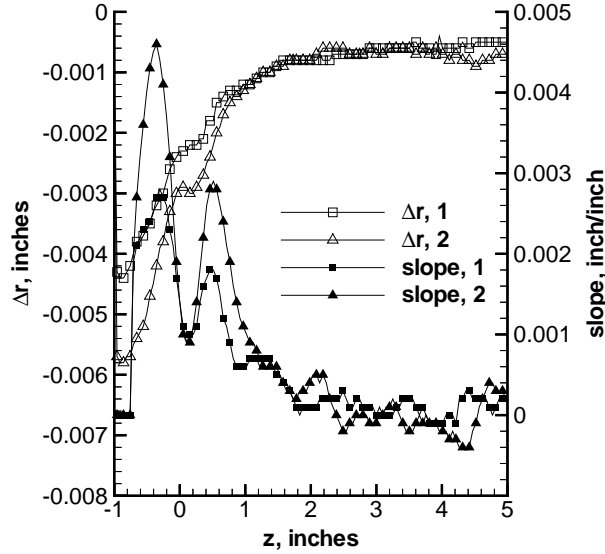


Figure 21: Excessive Waviness in Mandrel 1, After Polishing

eye are not always significant in size when examined under the microscope. These measurements confirm the problems with this mandrel, which is now useful only as scrap for a possible re-test of the grinding processes.

Nozzle Throat-Region Mandrel No. 3

Optimax for a third mandrel was ordered in October 1999, and arrived in December. This round also contains sufficient material for a witness specimen. The witness specimen is to be ground, inspected under the microscope, and polished, before grinding is carried out on the actual mandrel. In this way, process problems should be uncovered before the actual mandrel is irretrievably worked.

CONTRACTION MEASUREMENTS

Although the final inside contour of the nozzle sections cannot be completed until they can be matched to the final throat electroform, the contraction sections have been finished independently. Figure 26 shows the contraction assembly.

The upstream end of the contraction is at $z = -40.97$, where $z = 0$ at the throat. The joints on the inside surface are at $z = -40.970, -23.480, -6.265$, and -0.964 . The last joint is to the throat ring (see Fig. 25 in [46]). The downstream end of the throat-ring contour is at $z = -0.215$ in. The contraction was machined in sections, like the nozzle will be.

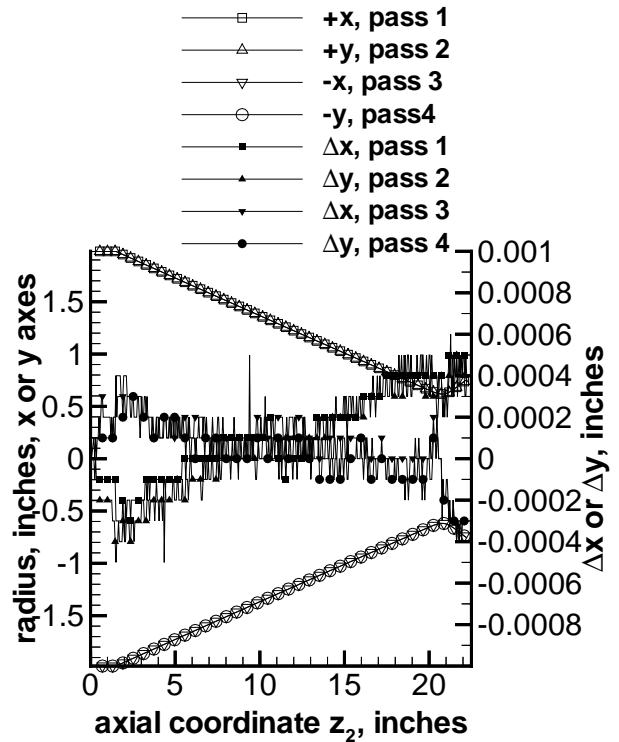


Figure 22: Contour Error in Mandrel 2, After Grinding

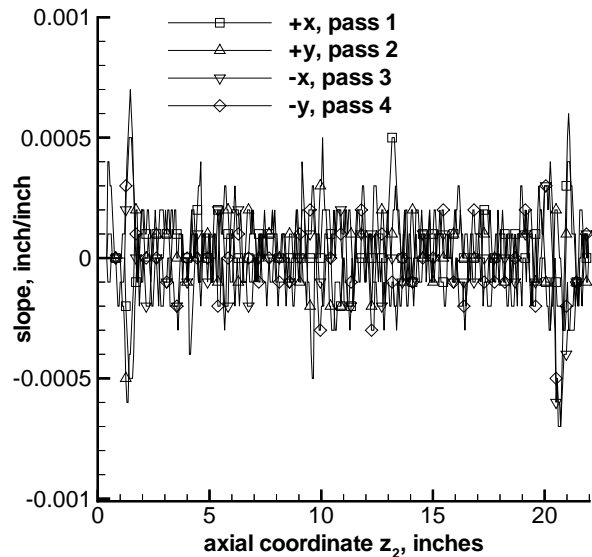
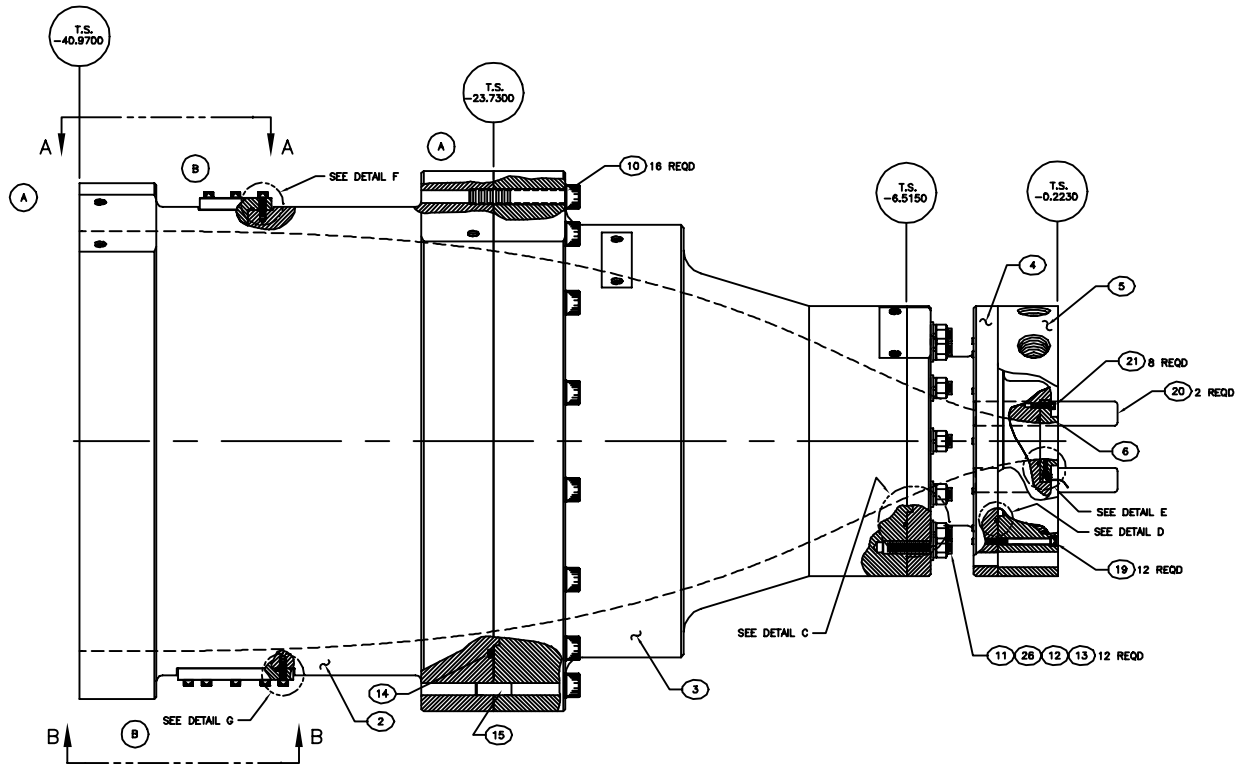


Figure 23: Waviness in Mandrel 2, After Grinding



-1 CONTRACTION SUB-ASSEMBLY Δ

Figure 26: Contraction Assembly. Scale: 1/8.

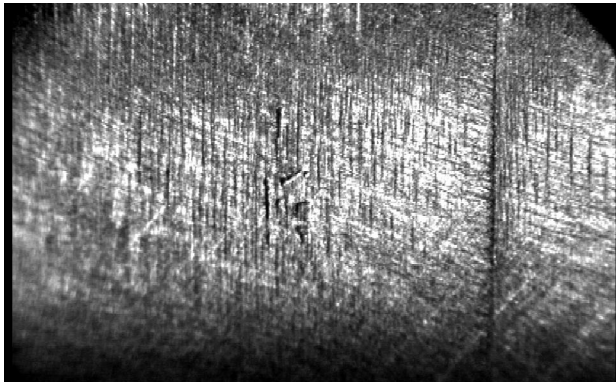


Figure 24: Gouges and Parting Line in Mandrel 2, After Test Polish

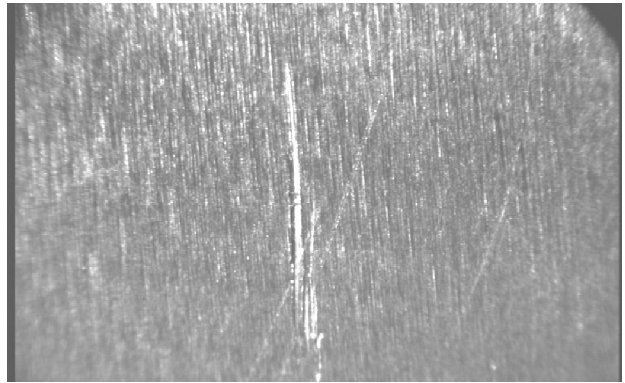


Figure 25: Large Gouge in Mandrel 2, After Test Polish

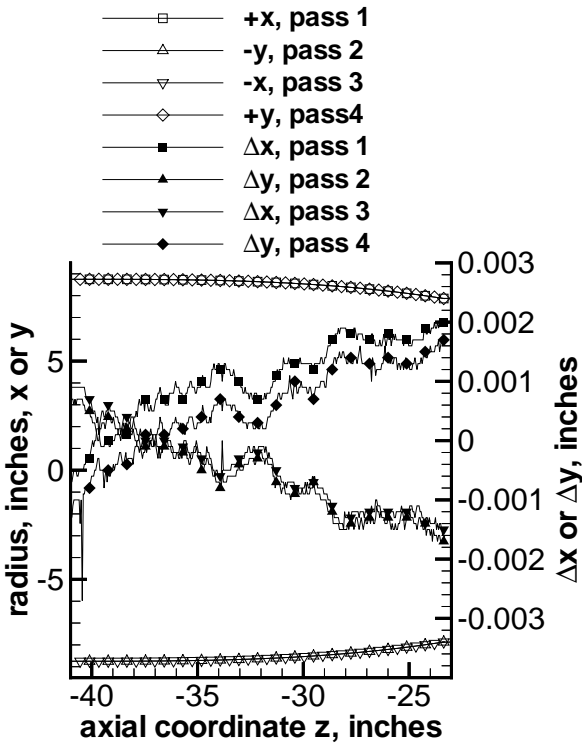


Figure 27: Contour of Contraction Section 1, Mated to Mid-Section

Figure 27 shows contour measurements on contraction section 1, taken on four rays at 90-deg. azimuthal intervals. The measurements were made with section 1 attached to the contraction mid-section, so the joint could be checked. The measurements extend from $z = -40.938$, just inside the entrance, to $z = -23.318$, just past the joint with the middle section. The radius is within ± 0.001 in. at the entry, but becomes oversize by about 0.002 inches near the joint. This is just within specification. Although there is no waviness specification on the contraction, the waviness slope is generally less than ± 0.001 inch/inch. The two spikes present near -40 and -33 inches are thought to be measurement errors, since they are present only on one ray and at one measurement station.

Figure 28 shows similar contour measurements on the throat section of the contraction. The throat ring was attached to the throat section, so the joint could be checked. The measurements extend from $z = -0.232$ to $z = -6.001$ in. The errors are all within ± 0.001 in., although there is a significant wave at about $z = -1$. This is near the joint between the machining of the throat ring and of the throat section. The slope here peaks at about 0.0018 inches,

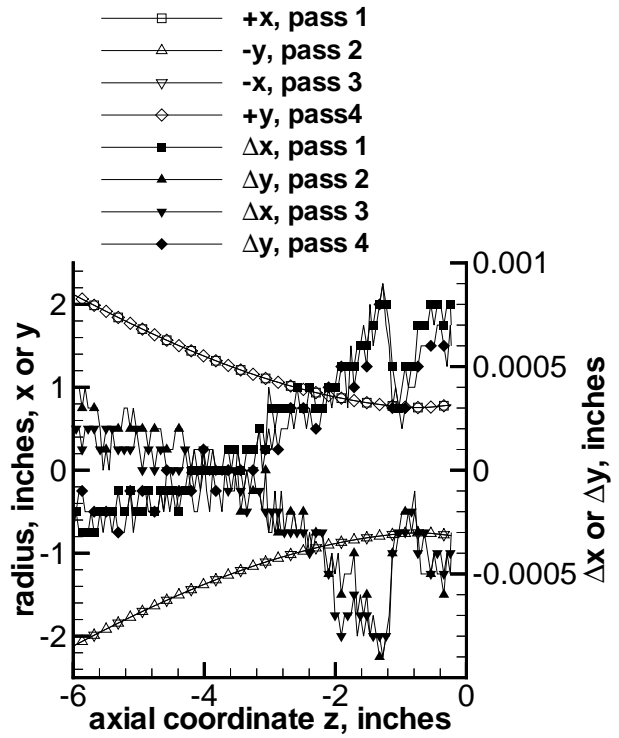


Figure 28: Contour of Contraction Throat Section, Mated to Mid-Section

which would be significant in the nozzle but is not in the contraction.

The last section to be cut was the middle section, which was faired to the upstream and downstream sections. In hindsight, this was not desirable, but it was done to speed shipment of contraction section 1 to Purdue. Figure 29 shows similar contour measurements, carried out with the throat section mated to the middle section. These measurements extend from $z = -1.02$ to $z = -23.448$ in. This measurement spans the joint at $z = -6.265$, and also the blend to the previous machining of the midsection entry, near $z = -23.4$. The deviations are generally within ± 0.001 in., for $z > -15$. There is a wave at $z = -6$, near the joint, but the amplitude is only about 0.001 inches. A larger wave is present near $z = -17$ in., for unknown reasons. The radius becomes nearly 0.002 inches undersize, between $z = -23$ and $z = -17$.

However, the most significant flaw is near the nozzle entry, as detailed in Fig. 30. It was almost impossible for the machinist to align the part in order to achieve near perfect blends both at the upstream and downstream ends of this cut. This was particularly true because there were no longer

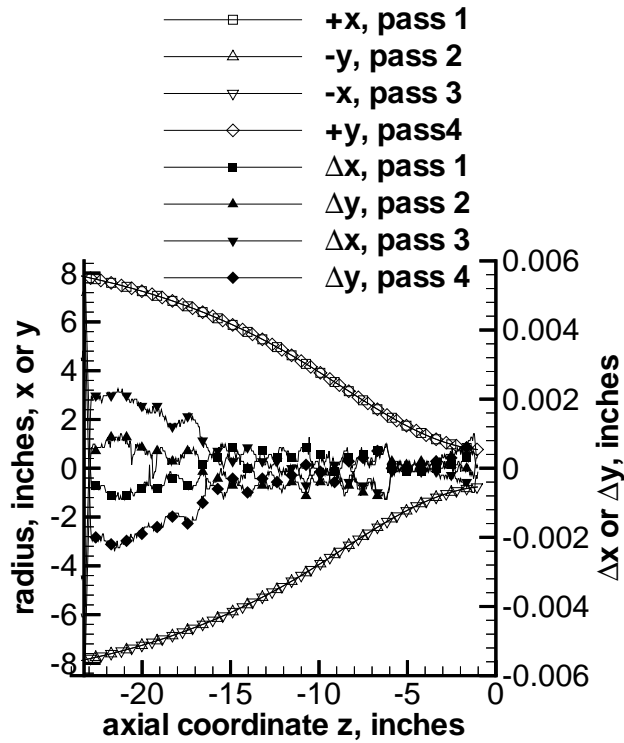


Figure 29: Contour of Contraction Midsection, Mated to Mid-Section

any flats for alignment, as the contour had already been machined in the earlier cuts. The machinist took special care to blend the downstream end, with good success as evident in Fig. 29. However, the upstream end has the large wave at $z = -23$ in., with an amplitude of about 0.006 in. and a slope of about 0.015 inch/inch. Although if such a wave was present in the nozzle, it would generate large Mach waves or perhaps trip the boundary layer, in the contraction the only risk is of a very small local boundary-layer separation. This risk was accepted, and no further machining is to be carried out on the contraction.

Clearly, the dual blend carried out in the last contraction machining is too difficult and risky. This means that none of the nozzle sections can be final machined until the throat is complete. Upon completion of the throat, each subsequent downstream section can be blend-machined, using the procedures developed on the test joint. Although all the nozzle sections are nearly complete, the final internal-contour cut must await completion of the throat section.

HEATING OF DRIVER-TUBE AIR

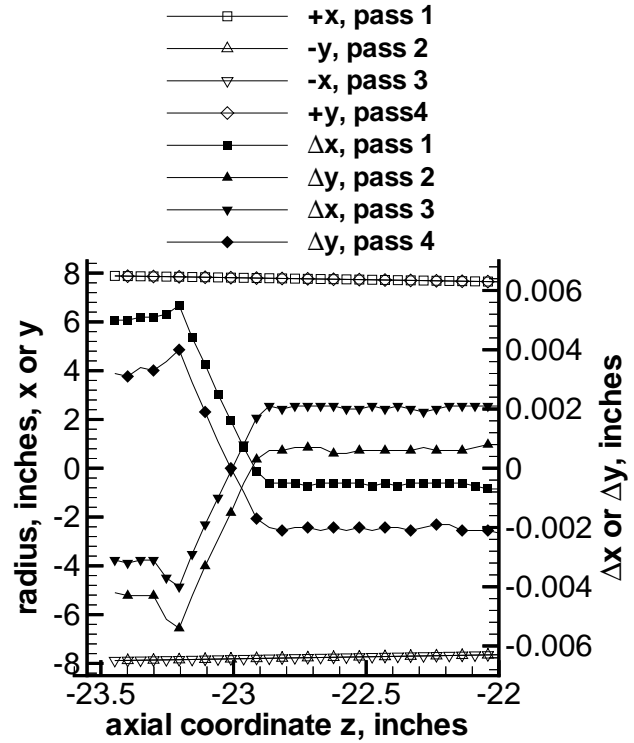


Figure 30: Detail of Contraction Midsection, Near Entry

Driver-Tube Heating

To avoid static liquefaction in the nozzle, at the maximum stagnation pressure of 300 psig (2.2 MPa, absolute), the driver-tube air must be heated to about 830R (370F or 460K or 190C) [61]. The driver tube is rated for 200C at 300 psig. It is made of 304 stainless steel, with a 17.5-inch inside diameter, and a 1/4-inch wall (Fig. 1). The resistance is about 0.003 ohms at room temperature. It is heated by passing approximately 2000A through it, at about 6V (as in Ref. [24]). Three large DC power supplies were obtained used, in order to supply this current (Electronic Measurements Inc., TCR10T750). A large aluminum I-beam is used as a return path, with the tunnel grounded near the nozzle so that current does not leak into the vacuum tank. An electrically-isolated flange is used to supply the air into the upstream end.

The thermocouple and control apparatus developed by Munro [59, 31] was moved to the new tunnel. Forty ungrounded type J thermocouples were installed, using band clamps [34]. To avoid the cold spots observed by Munro [31], the driver was mounted with insulated supports (Pipe Shields Inc.,

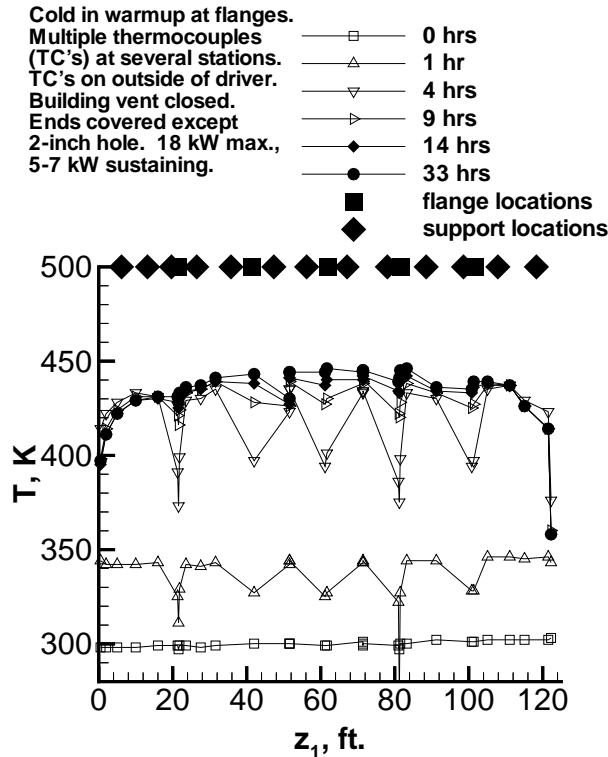


Figure 31: Driver-Tube Temperatures During Heating

Vacaville, CA, 3-inch insulation). Most of the supports are built to allow lengthwise movement on Teflon plates, to allow for thermal expansion, while restraining side-to-side motion. A fully insulated pipe anchor (Pipe Shields Inc.) was used to fix the driver tube near the nozzle end. The rest of the pipe was insulated with 3-inch fiberglass pipe insulation. The flanges were covered with fiberglass wrap and additional sections of large-diameter pipe insulation, 2 inches thick.

The driver tube was then heated to 160C [64]. The results are shown in Fig. 31. After about 4 hours of heating, the temperature nears the set-point of 433K. However, the flanges remain cold, because they act as heat sinks. After 14 hours, the flange temperatures equilibrate with the rest of the driver. There is little change at 33 hours. The ends of the tube are colder due to free convection, since they were uninsulated. The upstream end will not be important, since air from the upstream end will never enter the nozzle. The contraction on the downstream end will have special heaters, set to give an even temperature distribution. The support locations are not cold spots, proving the utility of the

insulated supports.

The RMS of the temperature deviations was about 7K after about 20 hours, a variation of roughly 2%. Recall that these thermocouples are placed on the outside of the driver tube, so the inner air temperature can be expected to be more uniform. In operation, the driver tube will be left hot whenever tunnel usage is expected. If hot air is added to the hot driver for each run, at roughly 1-hour intervals, Munro's results show that equilibrium can be reached in less than an hour [31].

After completion of the driver tube assembly, and attachment of contraction section 1, the driver tube will be wiped down like a clean room. A spelunker has been hired for this purpose. This is to ensure there are no particles to abrade the throat finish, trip the nozzle-wall boundary layer, or abrade the model or instrumentation.

Supply System for Hot Clean Air

Hot clean air needs to be supplied to the driver tube to give a rapid turnaround between runs, and to keep it free of particles. Air from the 50HP 145 psig automated compressor is passed through an after-cooler, a separator, two filters (Van-Air, Lake City, PA, grades C and RD), a holding tank, and an automated twin-tower dryer. It then enters 350 cubic feet of storage. Aftercooling to room temperature is an important part of helping the filters remove residual oil, which otherwise condenses in the throat of the wind tunnel and traps dust. The separator and filters have automatic drains.

This clean compressed air is then piped to the end of the driver tube. Here, it passes through three Van Air Filters, grades B, C, and RD, all operated in coalescing and particle-removal mode. The last of these increasingly fine filters is the RD, rated for particle removal down to 0.01μ , with 99.9999% efficiency of removal at 0.6μ , and a maximum oil carryover of 0.004 parts per million by weight. This last filter is downstream of the pressure regulator, which is remotely operable. The filters are not fitted with automatic drains, because the amount of material left to be filtered at this point is low. The filtering is carried out at room temperature because filters that are made for hot air are expensive and do not remove particles as well. Downstream of the last filter, all piping is stainless steel which has been specially cleaned out. No pipe dope is used on the joints, which are either welded or sealed with teflon tape. Welding must be carried out with care to avoid weld slag on the wetted surfaces.

The air is then heated in a stainless-steel circula-

tion heater (Heat Exchange and Transfer, Carnegie PA). A clean brass check valve is located upstream of the heater, to ensure that hot air cannot be pushed back into the filters. The 30kW electric heater is rated to heat 200-250 SCFM of air to 392F (200C) at 300 psig. It looks like a pipe with a side inlet and outlet; the heater rods are attached to a flange, and insert from one end. All wetted parts are stainless steel. The opposite end of the pipe is normally closed with a welded cap. However, to ensure that the heater could be cleaned of all weld slag and particles, the Purdue heater was fabricated with a blind flanged cover on the far end. The heater was carefully cleaned at the factory, and then further cleaned at Purdue. The hot air is piped to the driver through clean stainless piping, and a stainless-steel braided hose (to allow the 3-4 in. of flex needed when the driver tube expands while hot).

The heater has a thermocouple and standard controller, except for one custom option. A relay is fitted to the controls, to allow enabling or disabling the heating, remotely. After a run, cold air is first to be supplied to the driver, to raise the pressure to atmospheric, so the burst diaphragm can be changed. Then the heater is enabled remotely from the test area. It would normally then overheat, with no air flowing through it past the outlet thermocouple. After some small time to allow the rods to heat up, the air regulator will then be opened to start the airflow. When the driver is nearly up to the set pressure, this sequence of operations will be reversed. At a nominal operating pressure of 10 atm., most of the driver air will be supplied hot, and settings can be found to allow rapid equilibration with the driver tube temperature.

This system has been tested by blowing air into a clean lint-free cloth. The cloth is then inspected under a 40-power microscope to determine if any particles can be seen. A few particles were initially visible while the system was being blown clean. However, recent tests show none.

Operating Temperatures and Throat Heating

The static liquefaction limits for air are about 190C at 2.2 MPa (315 psia) or about 170C at 1.03MPa (150 psia); thus the driver tube is designed to allow heating to 200C. However, it is well known that air can be supercooled passing through the nozzle, without liquefaction [61]. The amount of supercooling has been very uncertain, for most tests do not detect the very low levels of nitrogen droplets that would damage a hot wire or bias an instability measurement, and supercooling also depends on

nozzle size.

This air temperature is a critical issue for the quiet-flow nozzle. This is because heating the throat above the stagnation temperature promises to provide markedly improved quiet-flow Reynolds numbers [47]. The throat of the tunnel can now only be heated to 450F (232C) maximum, for the metal sealing rings in the original design were replaced with silicone O-rings (Parker S604-70) to reduce leakage risk and save funds. There is thus very little margin for heating above the stagnation temperature needed to avoid static liquefaction.

However, recent instability experiments in the Mach-6 T-326 at ITAM, Novosibirsk, Russia, have been carried out at a stagnation temperature of 380K and a stag. pressure of 980 kPa (Alexander Shplyuk, private communication, Sept. 1999, also Ref. [13]). Shplyuk states that the minimum stagnation temperature to avoid noticeable condensation effects at the hot wire is about 350-360K. This suggests that our longer nozzle will be able to operate without condensation at perhaps 1.03 MPa and 380K (107C).

The nozzle throat is thus being fitted with a band heater and thermocouples (as in Fig. 25 of Ref. [46]), since it appears that the throat may be heated to nearly 100C above the stagnation temperature, without any part of the nozzle reaching above the O-ring maximum temperature. Thermocouples are being placed near the critical O-rings, so that experimental determination of the maximum throat temperatures can be made.

OTHER SYSTEMS

The burst-diaphragm system, vacuum system, and support structure are all in place and are being tested. The diffuser is complete and the second-throat section is nearly complete. These sections and the test results will be described in a future paper.

SUMMARY

Most of the Mach-6 Quiet-Flow Ludwig Tube at Purdue University has been completed. Tests have been carried out on the burst diaphragm system, the vacuum system, and the air supply and heating system. The contraction is nearly complete, and the nozzle has been machined (except for the final internal contour). Difficulties were experienced in fabricating a mandrel for the throat electroform. This mandrel must meet exceptional contour accuracy

specifications and be polished to a mirror finish. It requires exceptionally uniform material, with excellent grain structure and free of pits. Lessons learned from the problems with the first two mandrels are described in detail. The third mandrel is beginning fabrication. Initial tunnel operation is now planned for Fall 2000.

ACKNOWLEDGEMENTS

The research is funded by AFOSR under grants F49620-97-1-0037 and F49620-00-1-0016, monitored by Dr. Steve Walker. Fabrication of the tunnel was supported primarily by a gift from the Boeing Company and two grants from the Defense University Research Instrumentation Program (F49620-98-1-0284 and F49620-99-1-0278). The first grant was funded by AFOSR, and the second was funded jointly by AFOSR and BMDO. Tunnel completion is now also funded in part by contract BG-7114 from Sandia National Lab. The generous cooperation of Dr. Steve Wilkinson and the rest of the NASA Langley quiet tunnel group has been critical to our progress. Chris Tieche and Murthy Haradanahalli made the measurements with the Zygo optical profilometer.

Success in quiet-nozzle fabrication can only be achieved through the ideas, plans, and efforts of conscientious and highly skilled suppliers. The detailed design and fabrication of the nozzle and contraction is being carried out by Dynamic Engineering Inc., Newport News, Virginia. The design team was led by Mr. Doug Weber. Design modifications and fabrication process plans have been worked out with the help of Mr. Larry DeMeno, the program manager for the fabrication. Throat-mandrel polishing issues have been addressed using the expert advice of Mr. Paul Thomas at Optical Technologies, Franklin Park, Illinois.

References

- [1] AGARD. *Sustained Hypersonic Flight*, April 1997. CP-600, vol. 3.
- [2] J.B. Anders, P.C. Stainback, L.R. Keefe, and I.E. Beckwith. Fluctuating disturbances in a Mach-5 wind tunnel. *AIAA Journal*, 15(8):1123–1129, 1977.
- [3] I. Beckwith, F. Chen, S. Wilkinson, M. Malik, and D. Tuttle. Design and operational features of low-disturbance wind tunnels at NASA Langley for Mach numbers from 3.5 to 18. Paper 90-1391, AIAA, June 1990.
- [4] I. Beckwith, T. Creel, F. Chen, and J. Kendall. Freestream noise and transition measurements on a cone in a Mach-3.5 pilot low-disturbance tunnel. Technical Report NASA-TP-2180, NASA Technical Paper, 1983.
- [5] I.E. Beckwith, F.J. Chen, and T.R. Creel. Design requirements for the NASA Langley supersonic low-disturbance wind tunnel. Paper 86-0763, AIAA, 1986.
- [6] I.E. Beckwith and B.B. Holley. Görtler vortices and transition in wall boundary layers of two Mach-5 nozzles. Technical Paper 1869, NASA, 1981.
- [7] I.E. Beckwith, M.R. Malik, and F.-J. Chen. Nozzle optimization study for quiet supersonic wind tunnels. Paper 84-1628, AIAA, June 1984.
- [8] I.E. Beckwith and C.G. Miller III. Aerothermodynamics and transition in high-speed wind tunnels at NASA Langley. *Annual Review of Fluid Mechanics*, 22:419–439, 1990.
- [9] I.E. Beckwith and W.O. Moore III. Mean flow and noise measurements in a Mach-3.5 pilot quiet tunnel. Paper 82-0569, AIAA, March 1982.
- [10] Alan E. Blanchard, Jason T. Lachowicz, and Stephen P. Wilkinson. Performance of the NASA-Langley Mach-6 quiet wind tunnel. Paper 96-0441, AIAA, January 1996.
- [11] Alan E. Blanchard, Jason T. Lachowicz, and Stephen P. Wilkinson. NASA Langley Mach 6 quiet wind-tunnel performance. *AIAA Journal*, 35(1):23–28, January 1997.
- [12] A.H. Boudreau. Performance and operational characteristics of AEDC/VKF tunnels A, B, and C. Technical Report AEDC-TR-80-48, AEDC, July 1981. NASA citation 81N32161.
- [13] D.A. Bountin, A.N. Shilyuk, and A.A. Sidorenko. Experimental investigations of disturbance development in the hypersonic boundary layer on a conical models. In Saric et al., editor, *Laminar-Turbulent Transition. Proceedings of the IUTAM Symposium, Sedona*. Springer-Verlag, 1999. to appear.
- [14] D.B. Carver. Analytical investigation of flow quality in AEDC/VKF tunnel B – Mach 6 nozzle. Technical Memorandum AEDC-TMR-82-V24, AEDC, October 1982. Distribution lim-

- ited to US government agencies and their contractors.
- [15] F.-J. Chen, M.R. Malik, and I.E. Beckwith. Boundary-layer transition on a cone and flat plate at Mach 3.5. *AIAA Journal*, 27(6):687–693, 1989.
- [16] F.J. Chen, S.P. Wilkinson, and I.E. Beckwith. Görtler instability and hypersonic quiet nozzle design. Paper 91-1648, AIAA, June 1991.
- [17] T. R. Creel, I.E. Beckwith, and F.-J. Chen. Nozzle wall roughness effects on freestream noise and transition in the pilot low-disturbance tunnel. Technical Memorandum TM-86389, NASA, September 1985.
- [18] C.R. Fitch. Flow quality improvement at Mach 8 in the VKF 50-inch hypersonic wind tunnel B. Technical Report AEDC-TR-66-82, Arnold Engineering Development Center, 1966.
- [19] Wayne Z. Friend. *Corrosion of Nickel and Nickel-Base Alloys*. Wiley-Interscience, 1980.
- [20] Uwe G. Hingst. Laminar/turbulent flow transition effects on high speed missile domes. In *CP-493, Missile Aerodynamics*, pages 27–1 to 27–8. AGARD, 1990.
- [21] H.A. Korejwo and M.S. Holden. Ground test facilities for aerothermal and aero-optical evaluation of hypersonic interceptors. Paper 92-1074, AIAA, February 1992.
- [22] Dale W. Ladoon and Steven P. Schneider. Measurements of controlled wave packets at Mach 4 on a cone at angle of attack. Paper 98-0436, AIAA, January 1998.
- [23] Dale W. Ladoon, Steven P. Schneider, and John D. Schmisser. Physics of resonance in a supersonic forward-facing cavity. *J. of Spacecraft and Rockets*, 35(5):626–632, Sept.-Oct. 1998.
- [24] H. Ludwig, Th. Hottner, and H. Grauer-Carstensen. Der rohrwindkanal der aerodynamischen versuchsanstalt Gottingen. In *Sonderdruck aus dem Jahrbuch 1969 der DGLR*. DGLR, 1969.
- [25] G.A. Malone and D.M. Winkelman. High performance alloy electroforming. Contractor Report NASA-CR-183562, NASA, 1989. NASA STI 89N16041.
- [26] Dudley S. Marshall. Purdue quiet nozzle test section: Fabrication process. Technical Report Document D-686, DEI Task No. C038-001, DEI Model No. 922, Dynamic Engineering Inc., December 1998. Five pages including 3 figures. Obtain from S.P. Schneider, Purdue University.
- [27] Mark McCormick. Scanning electron microscope images of test mandrel. A 3-page informal report with 4 figures, 5 Oct. 1999. Obtain from S.P. Schneider, Purdue University.
- [28] J.R. Micol. Hypersonic aerodynamic/aerothermodynamic testing capabilities at Langley Research Center: aerothermodynamics facilities complex. Paper 95-2107, AIAA, June 1995.
- [29] J.R. Micol, R.E. Midden, and C.G. Miller III. Langley 20-inch hypersonic CF_4 tunnel: a facility for simulating real-gas effects. Paper 92-3939, AIAA, July 1992.
- [30] Raymond E. Midden and Charles G. Miller III. Description and calibration of the Langley hypersonic CF_4 tunnel. Technical Paper TP-2384, NASA, March 1995.
- [31] Scott Edward Munro. Effects of elevated driver-tube temperature on the extent of quiet flow in the Purdue Ludwig tube. Master's thesis, School of Aeronautics and Astronautics, Purdue University, December 1996. Available from the Defense Technical Information Center as AD-A315654.
- [32] S. R. Pate. Dominance of radiated aerodynamic noise on boundary-layer transition in supersonic/hypersonic wind tunnels. Technical Report AEDC-TR-77-107, Arnold Engineering Development Center, Arnold Air Force Station, TN, March 1978.
- [33] S.R. Pate and C.J. Schueler. Radiated aerodynamic noise effects on boundary-layer transition in supersonic and hypersonic wind tunnels. *AIAA Journal*, 7(3):450–457, March 1969.
- [34] Andrew Peters. Mach-6 Ludwig tube heating system, August 1998. A 5-page report with 3 figures. Obtain from S.P. Schneider.
- [35] A. Pope and K. Goin. *High-Speed Wind Tunnel Testing*. Wiley, New York, 1965.
- [36] H. Reed, R. Kimmel, D. Arnal, and S. Schneider. Drag prediction and transition in hypersonic flow. In *Sustained Hypersonic Flight*.

- AGARD, April 1997. Paper C15 in CP-600, vol. 3. Also appears as AIAA Paper 97-1818, June 1997.
- [37] Dan Ridefors. Letter from Uddeholm, Hagfors, Sweden, 9 Nov. 1999. Complaint No. 99-2536.
- [38] R. Rood, C. Griffith, and D. Engelhaupt. Mach 5 electroformed nickel nozzle refurbishment. Contractor Report CR-192421, NASA, 1993.
- [39] R. Rood, C. Griffith, D. Engelhaupt, and J. Cernosek. Mach 6 electroformed nickel nozzle refurbishment. Contractor Report CR-184299, NASA, 1992. NASA citation 92N21494.
- [40] Mario A. Rotea, Laura A. Randall, Ge Song, and Steven P. Schneider. Model identification of a Kulite pressure transducer. Paper 96-2278, AIAA, June 1996.
- [41] William H. Safranek. *The Properties of Electrodeposited Metals and Alloys*. American Electroplaters and Surface Finishers Society, Orlando, Florida, 1986. Second Edition.
- [42] Terry R. Salyer, Laura A. Randall, Steven H. Collicott, and Steven P. Schneider. Use of laser-differential interferometer to study receptivity on a hemispherical nose at Mach 4. Paper 98-0238, AIAA, January 1998.
- [43] J.D. Schmisser, Steven H. Collicott, and Steven P. Schneider. Laser-generated localized freestream perturbations in supersonic/hypersonic flows. Paper 98-2495, AIAA, June 1998.
- [44] J.D. Schmisser, J.O. Young, and S.P. Schneider. Measurement of boundary-layer transition on the flat sidewall of a rectangular Mach-4 quiet-flow nozzle. Paper 96-0852, AIAA, January 1996.
- [45] S. P. Schneider and C. E. Haven. Quiet-flow Ludwig tube for high-speed transition research. *AIAA Journal*, 33(4):688–693, April 1995.
- [46] Steven P. Schneider. Design and fabrication of a 9-inch Mach-6 quiet-flow Ludwig tube. Paper 98-2511, AIAA, June 1998.
- [47] Steven P. Schneider. Design of a Mach-6 quiet-flow wind-tunnel nozzle using the $e^{**}N$ method for transition estimation. Paper 98-0547, AIAA, January 1998.
- [48] Steven P. Schneider. Measurements of roughness and waviness on the quiet-nozzle test joint, September 1998. A 5-page informal report with 26 figures. Obtain from the author.
- [49] Steven P. Schneider. Flight data for boundary-layer transition at hypersonic and supersonic speeds. *Journal of Spacecraft and Rockets*, 36(1):1–13, 1999.
- [50] Steven P. Schneider. Trinocular microscope images of mandrel no. 2: Tests of the 15-5PH mandrel for Mach-6 quiet-flow nozzle throat, December 1999. A 10 page informal report with 9 figures. Obtain from the author.
- [51] Steven P. Schneider. Zygo optical profilometer measurements of hard nickel coupon: Sample tests for the Mach-6 quiet-flow nozzle throat, May 1999. A 6 page informal report with 10 figures. Obtain from the author.
- [52] Steven P. Schneider. Zygo optical profilometer measurements of soft nickel coupon: Sample tests for the Mach-6 quiet-flow nozzle throat, May 1999. A 19 page informal report with 29 figures. Obtain from the author.
- [53] Steven P. Schneider. Zygo optical profilometer measurements of test-mandrel electroform: Post-heating results, August 1999. A 17 page informal report with 32 figures. Obtain from the author.
- [54] Steven P. Schneider. Zygo optical profilometer measurements of test-mandrel electroform: Pre-heating results, July 1999. A 21 page informal report with 35 figures. Obtain from the author.
- [55] Steven P. Schneider. Zygo optical profilometer measurements of test mandrel: Following regrinding and repolishing, December 1999. A 10 page informal report with 17 figures. Obtain from the author.
- [56] Steven P. Schneider. Zygo optical profilometer measurements of test mandrel: Sample tests for the Mach-6 quiet-flow nozzle throat, June 1999. A 13 page informal report with 22 figures. Obtain from the author.
- [57] Steven P. Schneider, Steven H. Collicott, J.D. Schmisser, Dale Ladoon, Laura A. Randall, Scott E. Munro, and T.R. Salyer. Laminar-turbulent transition research in the Purdue

- Mach-4 quiet-flow Ludwieg tube. Paper 96-2191, AIAA, June 1996.
- [58] Steven P. Schneider, Christine E. Haven, Joseph B. McGuire, Steven H. Collicott, Dale Ladoon, and Laura A. Randall. High-speed laminar-turbulent transition research in the Purdue quiet-flow Ludwieg tube. Paper 94-2504, AIAA, June 1994.
- [59] Steven P. Schneider and Scott E. Munro. Effect of heating on quiet flow in a Mach 4 Ludwieg tube. *AIAA Journal*, 36(5):872–873, May 1998.
- [60] C.J. Schueler. An investigation of model blockage for wind tunnels at Mach numbers 1.5 to 19.5. Technical Report AEDC-TN-59-165, Arnold Engineering Development Center, February 1960. DTIC citation AD-232492. Limited distribution.
- [61] P.P. Wegener and L.M. Mack. Condensation in supersonic and hypersonic wind tunnels. *Advances in Applied Mechanics*, 5:307–447, 1958.
- [62] S. P. Wilkinson, S. G. Anders, and F.-J. Chen. Status of Langley quiet flow facility developments. Paper 94-2498, AIAA, June 1994.
- [63] S.P. Wilkinson, S.G. Anders, F.-J. Chen, and I.E. Beckwith. Supersonic and hypersonic quiet tunnel technology at NASA Langley. Paper 92-3908, AIAA, July 1992.
- [64] Fuguo Zhou. Temperature measurement from heating the driver tube of the Mach-6 Boeing Ludwieg tube, May 1999. A 32-page report with 12 figures. Obtain from S.P. Schneider.